AWARD NUMBER: W81XWH-12-1-0542

TITLE: Novel in Vitro Modification of Bone for an Allograft with Improved Toughness Osteoconductivity

PRINCIPAL INVESTIGATOR: Yener N. Yeni, Ph.D.

CONTRACTING ORGANIZATION: Henry Ford Health System, Detroit, MI 48202

REPORT DATE: June 2015

TYPE OF REPORT: Final

PREPARED FOR: U.S. Army Medical Research and Materiel Command
Fort Detrick, Maryland 21702-5012

REPORT DOCUMENTATION PAGE

Form Approved
OMB No. 0704-0188

1. REPORT DATE	2. REPORT TYPE	3. DATES COVERED
June 2015	Final	30 Sep 2012 – 29 June 2015

4. TITLE AND SUBTITLE
Novel in Vitro Modification of Bone for an Allograft with Improved Toughness Osteoconductivity

5a. CONTRACT NUMBER
W81XWH-12-1-0542

5b. GRANT NUMBER

5c. PROGRAM ELEMENT NUMBER

6. AUTHOR(S)
Yener N. Yeni

E-Mail: yeni@bjc.hfh.edu

5d. PROJECT NUMBER

5e. TASK NUMBER

5f. WORK UNIT NUMBER

7. PERFORMING ORGANIZATION NAME(S) AND ADDRESS(ES)

HENRY FORD HEALTH SYSTEM
1 FORD PL ST E5F
DETROIT MI 4822-3450

8. PERFORMING ORGANIZATION REPORT NUMBER

9. SPONSORING / MONITORING AGENCY NAME(S) AND ADDRESS(ES)
U.S. Army Medical Research and Materiel Command
Fort Detrick, Maryland 21702-5012

10. SPONSOR/MONITOR'S ACRONYM(S)

11. SPONSOR/MONITOR'S REPORT NUMBER(S)

12. DISTRIBUTION / AVAILABILITY STATEMENT
Approved for Public Release; Distribution Unlimited

13. SUPPLEMENTARY NOTES

14. ABSTRACT
The purpose of the project is to investigate a potential application of ALT-711 (4,5-Dimethyl-3-(2-oxo-2-phenylethyl)-thiazolium chloride) in improving both mechanical and biological quality of femoral cortical bone for the purpose of providing better allograft materials via chemically breaking down AGEs (Advanced Glycation Endproducts) in the bone matrix. AGEs are naturally accumulated with age in connective tissues and believed to have adverse effects on the biological and mechanical functions. Thus allografts sourced from bones with a high level of AGEs are likely to have a higher risk of nonunion and premature failure in the hosts. The current scope, as a proof of concept study, is to measure the effectiveness of ALT-711 on both cellular and mechanical characteristics of bones with and without prior glycation treatment (an artificial method to increase AGEs). Effects of ALT-711 on osteogenic expression of stem cells on the bone substrates, cell division, apoptosis and mineralization as well as the R-curve parameters including crack propagation, fracture toughness and critical crack length were measured. We found that the crosslink breaker ALT-711 can modify bone matrix, affect its fracture behavior and affect stem cell differentiation when used to treat allograft bone. However, these effects were not uniform enough that the proposed crosslink breaking method can be directly translated in to a protocol for enhancement of allograft performance. Further understanding of the complex interactions among donor age, sex and the AGE type would be necessary to develop more effective approaches to selectively remove the relevant AGEs from the tissue. Such understanding may also be key to understanding age related bone fragility and the sex disparity in fracture risk.

15. SUBJECT TERMS
Fracture healing, allograft bone, nonenzymatic glycation crosslinks, crosslink breaker, osteoconductivity, stem cell culture, fracture mechanics

16. SECURITY CLASSIFICATION OF:			17. LIMITATION OF ABSTRACT	18. NUMBER OF PAGES	19a. NAME OF RESPONSIBLE PERSON
a. REPORT	b. ABSTRACT	c. THIS PAGE			USAMRMC
U	U	U	UU	37	19b. TELEPHONE NUMBER *(include area code)*

TABLE OF CONTENTS

1. INTRODUCTION

Bone grafts are used to provide mechanical support and enhance the biological repair of skeletal defects. Age-related increase of advanced glycation endproducts (AGEs) within the collagen network of skeletal tissues adversely affects the mechanical and biological qualities of the allograft tissue. It is hypothesized that treatment with an AGE-breaker compound will increase fracture resistance and osteoconductivity of an allograft. Objectives are 1) to investigate the extent to which in vitro treatment of human cortical bone with an AGE-breaker will improve the fracture toughness of the tissue by treating normal and artificially glycated tissues in different concentrations of ALT-711 (4,5-Dimethyl-3-(2-oxo-2-phenylethyl)- thiazolium chloride) solutions followed by mechanical testing; 2) to investigate the extent to which in vitro treatment of young and old femoral cortical bone with an AGE-breaker will affect the recruitment, division and osteogenic development of mesenchymal stem cells by using normal and artificially glycated demineralized bone samples (treated or non-treated with ALT-711) in a cell culture. The degree of cell proliferation was determined by ethynyl deoxyuridine incorporation, apoptosis by Hoechst nuclear staining, osteogenic differentiation by Alizarin staining for mineral deposition, and alkaline phosphatase activity and expression of bone-characteristic genes, osteocalcin, Runx2, and col1a1 by RT-PCR. Spectrophotometry and fluorescence microscopy were used to quantify AGEs.

2. KEYWORDS

Fracture toughness, R curve, advanced glycation end products, femoral cortical bone, ALT711

3. OVERALL PROJECT SUMMARY

The following table summarizes the tasks performed in this project (**Table 1**).

Table 1. Summary of project tasks

Tasks	Description	Status
Task 1	Retrieval of 24 femurs	Completed ✓
Task 2	Optimize AGE-breaker (ALT-711) treatments	Completed ✓
Task 3	Preparation of test samples	Completed ✓
Task 4	Mechanical testing	Completed ✓
Task 5	Preparation of bone substrates and running cell cultures	Completed ✓
Task 6	Measure cell division (ethynyl deoxyuridine)	Completed ✓
Task 7	Measure apoptotic cell density (Tunel)	Completed ✓
Task 8	Measure mineral nodules (Von Kossa/histochemical)	Completed ✓
Task 9	Measure expression of osteogenic markers (alkaline phosphatase, osteocalcin, RUNX2 and COL1A1)	Completed ✓
Task 10	Data analysis, publications, reports	Completed ✓

Task 1. Retrieval of 24 cadaveric human fresh-frozen femurs from tissue banks and body donation programs. (Months 1-4.)

1a. Review and activation of tissue collection protocols by the donation program (Month 1).
1b. Collection and shipment of the femurs. (Months 1-4.)

Approval of the institutional review board (IRB 7511) for the project was obtained and submitted to the USAMRMC Office of Research Protections (ORP), Human Research Protection Office (HRPO) for the review along with a claim of exemption from the review to use preexisting cadaveric femurs. The statement that the project may proceed with no further requirement for review by the HRPO was received prior to the beginning of the supported period. In accordance with this notification (HRPO Log Number A-17384), newly retrieved femurs as well as previously existing deidentified cadaveric femurs are used.

As previously proposed, through approved tissue banks (the National Disease Research Interchange (NDRI), Platinum Training, and LifeLegacy Foundation) we obtained all required femurs meeting age, sex and medical condition criteria. The procurement of femurs took longer than initially planned as healthy donors are often prioritized for transplant surgeries. We therefore revised some of the exclusion criteria, taking into account similar work done by Wu et al. [1] and feedback from the tissue bank (**Table 2**) so as to increase the chance of procurement without sacrificing the intention of the criteria.

Table 2. Exclusion criteria presented in this table were revised to increase the chance of procurement and reduce miscommunication with the tissue providers without sacrificing the intention of the criteria.

	Original criteria	**New criteria**
Post mortem to inventory (PMI) time	24 hr	72 hr
Bed rest prior to death	Ventilated state	Over 6 weeks
History of radiation or chemotherapy	Any history of radiation or chemotherapy	Last five years before death
Medication	Anticonvulsant	-
Disease/conditions	-	Osteogenesis imperfecta, Cushing's syndrome, Syphilis

Task 2. Optimize AGE-breaker (ALT-711) treatments (36 sections/femur; 4 distal femurs. (Months 1-4.)

2a. Preparation of thin bone sections from femurs and demineralization in EDTA solutions. (Month 1.)
2b. Artificial glycation in ribose and ALT-711 treatment of the normal and glycated subgroups (0, 0.3mM and 3mM; 0, 5, 10, 20 hour groups). (Month 1-2.)
2c. Fluorescence analysis of AGE content. (Month 2-4.)

Although the original proposal for determining the optimal ALT treatments was about demineralized bone samples to be used as substrates in Aim 2, we felt that additional experiments needed to be performed to optimize the treatment for undemineralized specimens of Aim 1. We have taken two approaches in the analysis of fluorescence, one using spectrophotometry and another using fluorescence microscopy.

i) Initial spectrophotometry experiments with powderized bone

In order to relate fluorescence readings from the spectrophotometer to a known standard, a quinine reference standard was developed. Various concentrations of quinine were prepared in 100 ml sample volumes. A linear relationship between fluorescence and concentrations of quinine was found (**Figure 1**), which would allow presentation of arbitrary units of fluorescence in equivalent ng/mL quinine.

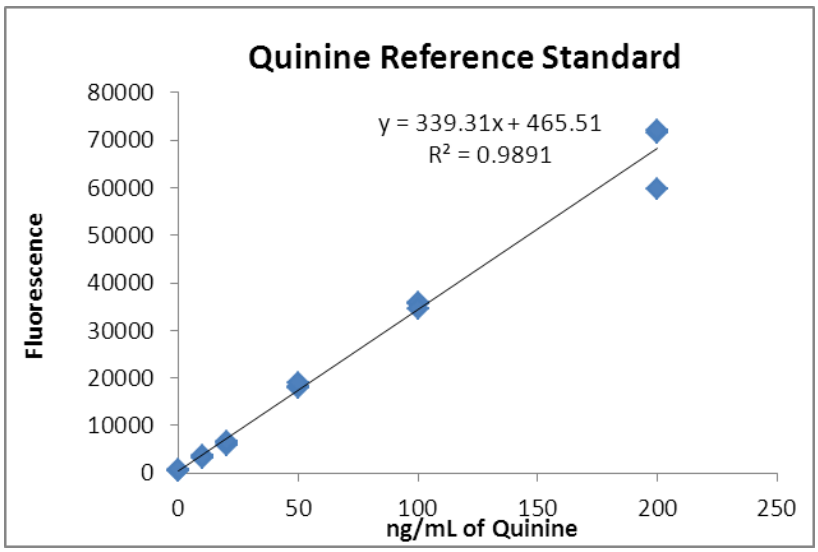

Figure 1: As expected, a strong linear relationship was established between arbitrary units of fluorescence and quinine concentrations. This relationship was intended to serve as a standard for quantification of fluorescence in our spectrophotometric approach.

For the initial studies to frame an appropriate range of bone powder concentration, ALT concentration, and treatment duration, an approximately 2x2 cm section of a distal diaphysis was powdered to be used as a uniform reference. Our assumption was that the powder was sufficiently homogeneous to be used as a standard "bone"

material. The decalcified specimens were digested in papain (+ Tris buffer) with 24 hours of incubation at 55 ºC and prepared into 10, 25, 50 and 100 mg powders in 1 ml digestion solution. In order to determine the extent to which the digestion solution fluoresces, papain + Tris buffer was also measured before and after 24 hour incubation at 55 ºC. We found that fluorescence and bone powder concentration had a linear relationship. All powder weights except 100 mg were within the range of the quinine standard established above.

A slight decrease in fluorescence was observed with increasing ALT concentration (**Figure 2**). However, compared to the bone's fluorescence, the background fluorescence occurred from the buffer and ALT treatment solution was small. We concluded that the fluorescence from the digestion or ALT solution is not high enough to prevent us from measuring variations in bone. The results from a series of experiments were consistent in that 3 mM ALT at 70 hours or more duration is an effective treatment (**Figure 3**), while less than 0.3 mM is not effective and 10 mM did not increase the fluorescence (**Figure 4**). In conclusion, 3 mM for about one week appears adequate but the duration of the treatment must be controlled.

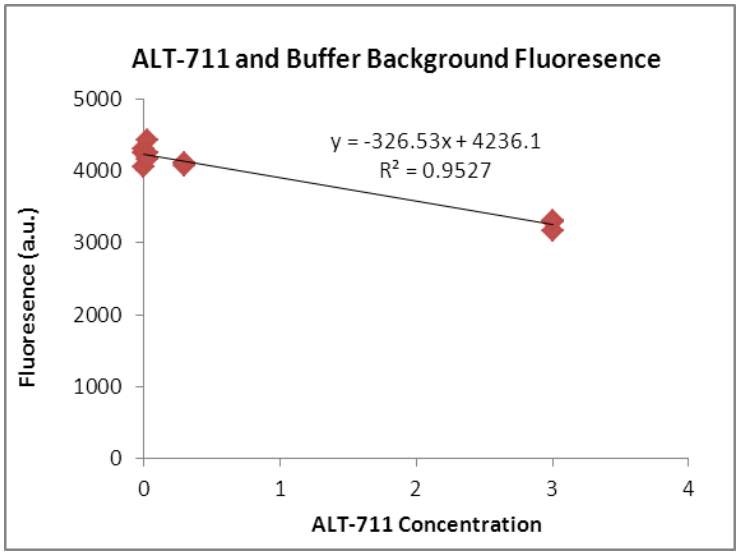

Figure 2: Fluorescence from the ALT treatment solutions at 7 days.

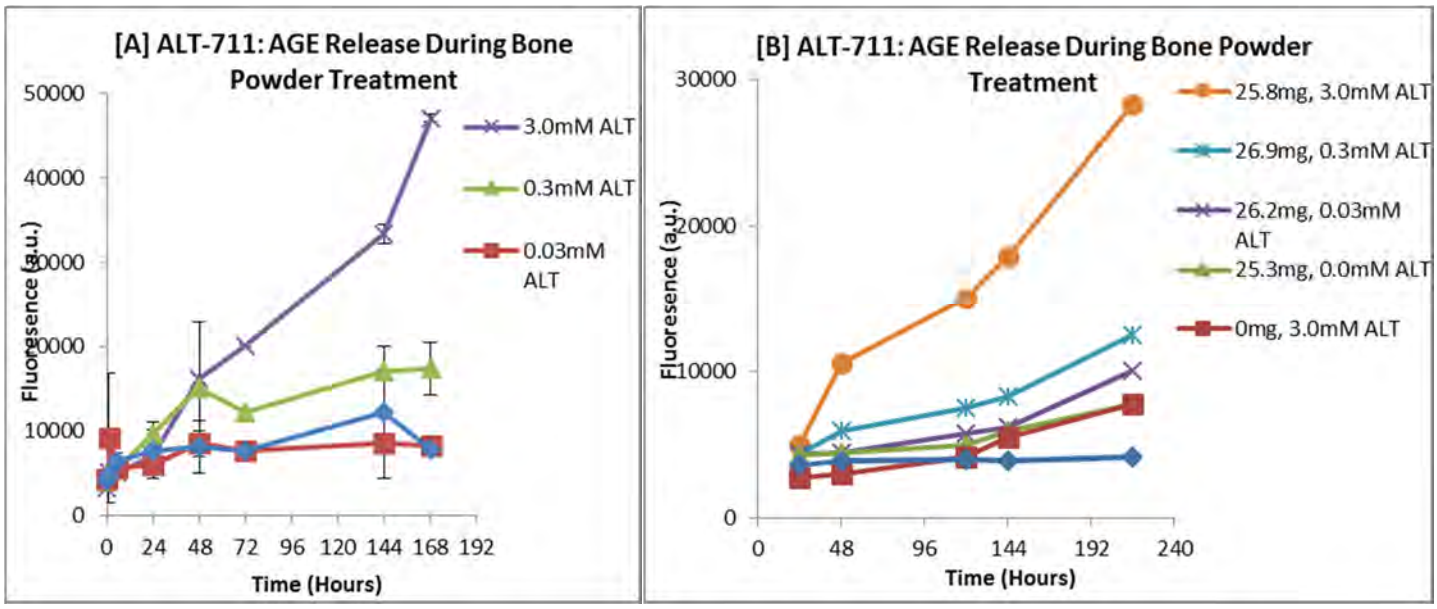

Figure 3: Results from typical series of experiments ((A) and (B)) in which the effect of time and dosage is examined. (A) These results suggest that at least 70 hours treatment in 3 mM ALT is necessary to observe an effect. The error bars represent the standard deviation within triplicate measurements. (B) Another experiment using 30 mg bone powder, which is in general agreement with (A) that 3 mM is effective.

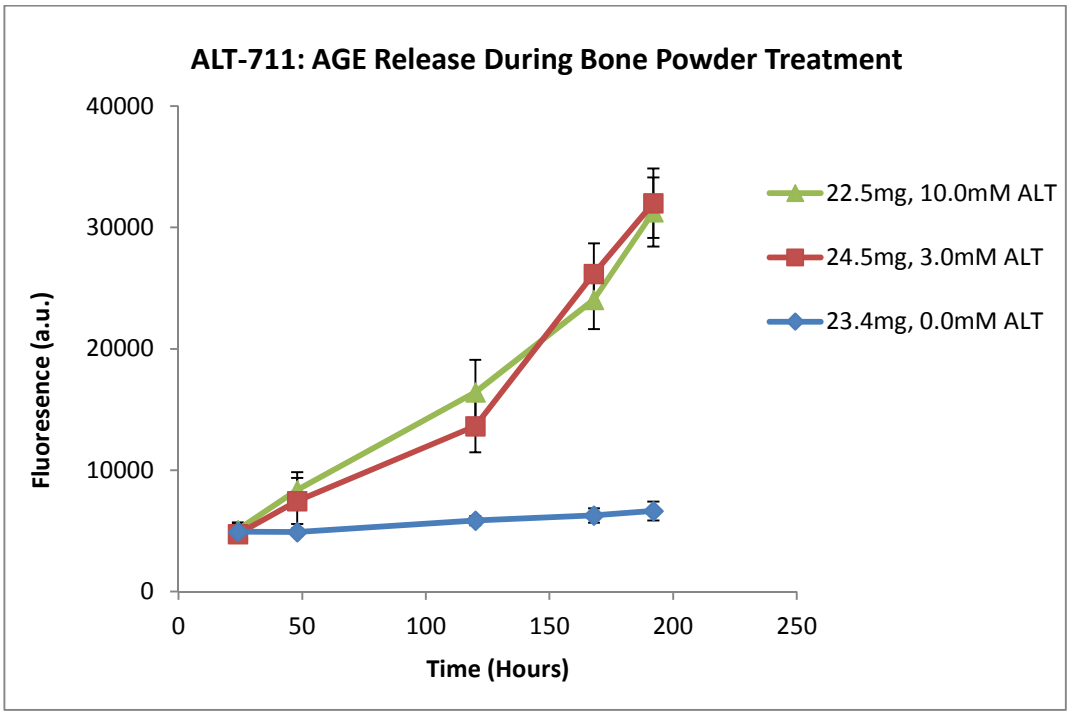

Figure 4: The experiment in **Figure 3B** was repeated with ALT concentrations of 3 mM and 10 mM to examine if the concentration of ALT was too low to be able to determine differences between the treatment concentrations. The fluorescence levels after 50 to ~200 hours were higher in treatment groups than no treatment, but the 3 mM and 10 mM groups didn't appear different.

ii) Epi-fluorescence microscopy with demineralized bone

The epi-fluorescence microscopy method has two main advantages over the spectrophotometry method in detecting relative changes in AGE concentration; i) it is a non-destructive method, and thus a longitudinal observation of changes in AGE concentrations within each sample is possible, and ii) it provides a visual distribution of AGEs across the area of examination (**Figure 5**).

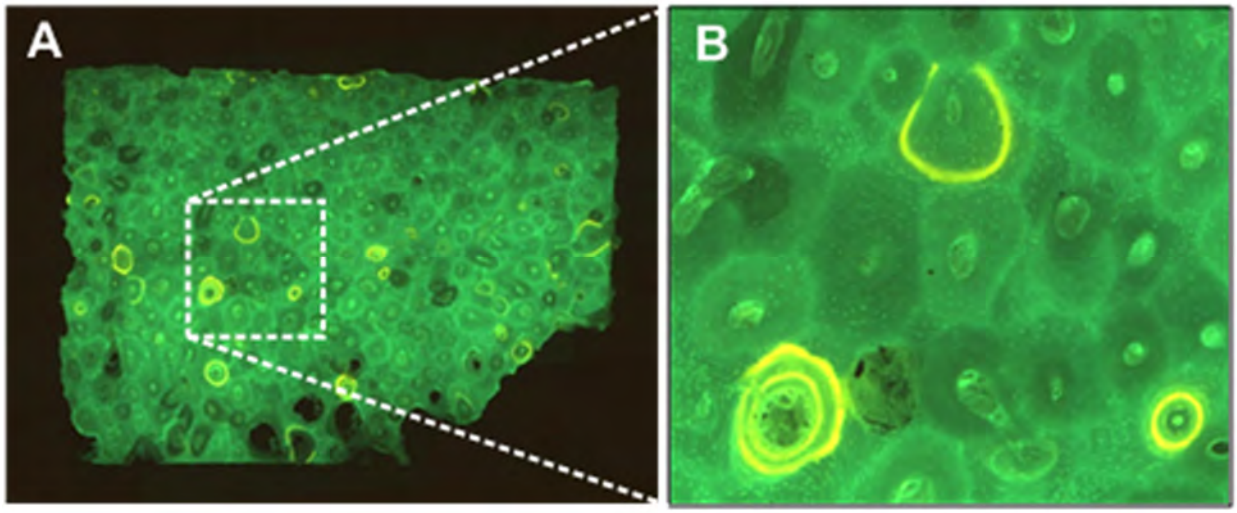

Figure 5: (A) A ~100 µm thick human femoral bone section (undecalcified) under epi-fluorescence microscopy and (B) a subregion of the section showing a magnified view of the haversian system. Osteons with lower fluorescence are younger (recently formed) while those with brighter fluorescence (due to higher AGE content) are older. Green-yellow concentric rings found around osteons are residues, possibly from antibacterial treatments (tetracycline) while the donor was still alive.

We prepared 20 femoral bone sections with thickness of 110 ± 15 µm using a circular diamond saw (South Bay, San Diego) under constant water irrigation to prevent heat damage to the tissue. A femoral bone piece (a 61 year old male donor) was aligned so that sections would reveal the axial plane (transverse to the supero-inferior direction) of the femur. The processed thin sections were further trimmed into a rectangular shape (approximately 5 mm x 4 mm) using a scalpel blade and a corner was also notched to create a landmark for a reference for longitudinal imaging (**Figure 5**). The 20 sections were divided into five treatment groups (**Table 3**) and PBS

buffer together with chloroform (20 µL/25 mL) and gentamicin (25 µL/25 mL) to inhibit fungal and bacterial growth during 33 days of incubation (37 °C).

Before EDTA decalcification, they were individually wet mounted and photographed under epi-fluorescence microscopy (Nikon Corp., Tokyo, Japan) using a x4 objective with 60 ms exposure time. The light source was ultraviolet (UV) through 400±440 nm excitation and 480 nm barrier filters. Sections were decalcified for 50 hours and then another set of images were taken for day 0 reference. Longitudinal fluorescence imaging was carried out every 2-3 days up to two weeks and then weekly thereafter up to 33rd day (**Figure 6**).

Table 3. Description of the treatment groups. Each treatment group included 4 sections.

Treatment group notation	Followup treatment	Description	Treatment solution	Storage temp	Duration
GLY	GLY → ALT(n=2) GLY → PBS(n=2)	Initially glycated only but later divided into two groups GLY→ALT and GLY→PBS at day 22.	Ribose (666 mM) ALT-711 (3 mM) PBS	37 °C	GLY = 22 days ALT = 11 days PBS = 11 days
GLY+ALT		Glycated for 7 days and then ALT	Ribose (666 mM) ALT-711 (3 mM)	37 °C	GLY = 7 days ALT = 26 days
ALT		ALT-711 only	ALT-711 (3 mM)	20 °C	33 days
C		Control – no treatment	PBS	20 °C	33 days
F		Frozen control – no treatment and kept in a freezer	PBS	-20 °C	33 days

We observed a rapid increase in fluorescence levels in glycated specimens (**Figures 6-7**), however when ALT-711 was introduced in the GLY+ALT group at day 7, the increase in FL from the previous glycation treatment was reversed, reducing FL by 15%. However, after day 13 a slow but steady increase in FL could be observed again. In GLY specimens, ALT-711 treatment was introduced to 2 of 4 GLY sections at day 22 while the other 2 sections were placed in PBS solution to confirm the ALT's effect in reducing FL observed in the GLY+ALT group between day 7 and 13. At this point, all four GLY sections were at a nearly saturated state from 22 days of GLY treatment. Upon ALT-711 treament on the GLY saturatrated sections, the FL decreased at day 27 and then further decreased up on a replenishment of ALT-711 solution at day 29, resulting in a total decrease of 14%.

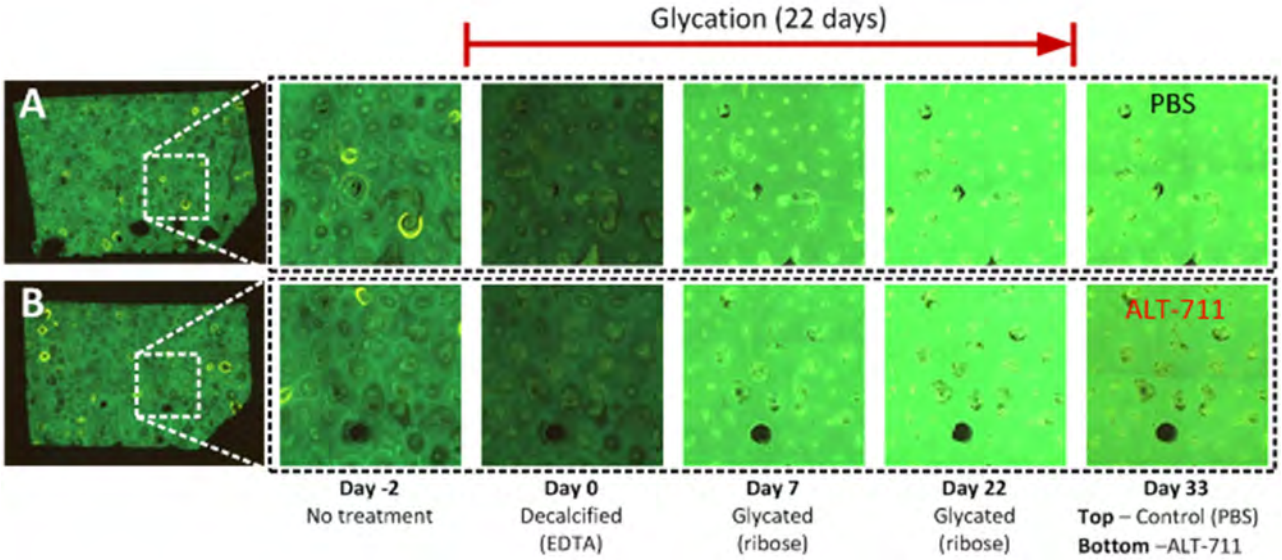

Figure 6: Longitudinal changes of fluorescence level (FL) from decalcification, glycation and ALT-711 treatments. Both (A) and (B) show steady increase of FL during glycation up to 22nd day. The FL is lower after 11 days of ALT-711 treatment (Day 33) than at 22nd day of glycation (B) while no clear difference was observed after 11 days of PBS treatment (control) following the 22 day glycation regimen (A).

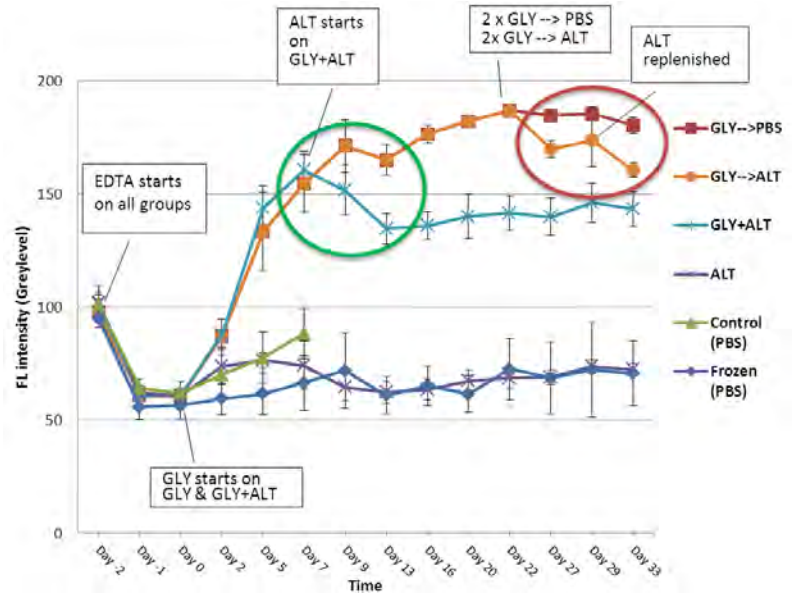

Figure 7: Longitudinal changes in average fluorescence level (FL) for each group during decalcification, glycation and ALT-711 treatments. A marked drop in FL can be observed for the GLY+ALT group during the period from day 7 to 13 (green circle) and for the GLY→ALT group during the period from day 22 to 33 (red circle). Error bars indicate standard deviations.

The ALT group, where ALT-711 was immediately applied to freshly decalcified sections, did not show a difference from the control groups.

In order to confirm the ability of ALT-711 to reverse the increased FL by ribose glycation, we conducted another similar experiment with 40 bone sections from a single donor, allocating 10 sections to each group (i.e. GLY→PBS, GLY→ALT, ALT, PBS control). In this experiment all four groups were subjected to a 37 °C incubation condition as opposed to the previous experiment, in which the ALT and control groups were kept at room temperature. As in the previous experiment, we observed a marked decrease (-20%) in FL levels that were initially raised by glycation (GLY→ALT, $p<0.0048$) relative to the group that was treated with PBS after glycation (GLY→ PBS; control). Additionally, no substantial differences were observed in the ALT and control groups over the 14 day period (**Figure 8**).

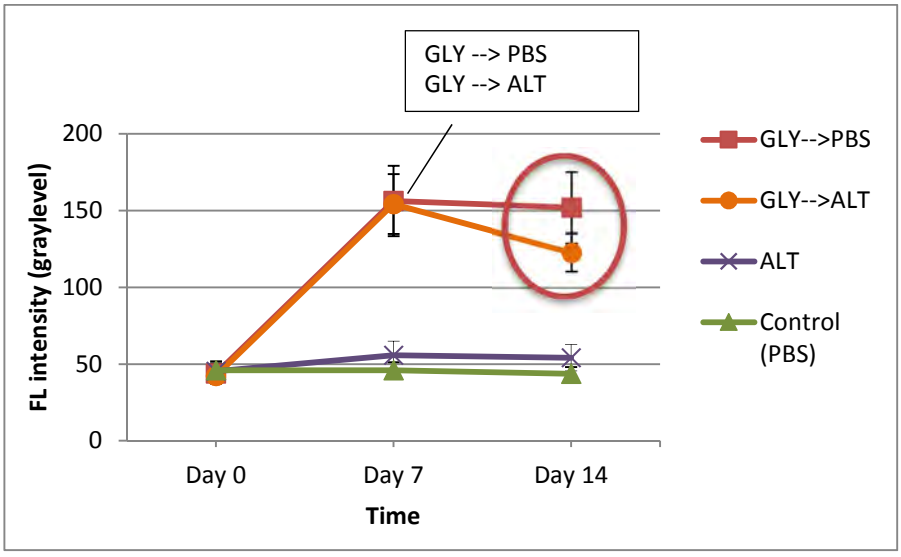

Figure 8: Both GLY→PBS and GLY→ALT groups have identically increased their FL at day 7 by glycation and there is a subsequent decrease from ALT-711 in GLY→ALT while no significant change is seen in GLY→PBS. Both ALT and PBS control groups did not change their FL significantly over the 14 day period. This experiment confirms that ALT-711 has a significant reducing effect on FL in previously glycated samples.

The results of both experiments suggest that ALT-711 of 3 mMol concentration over 7 day application has a significant effect on reducing the level of fluorescence intensity (i.e., AGE content) previously increased by ribose glycation ($p < 0.0048$). However, after day 7, its potency is reduced and further replenishment of the solution was needed. This suggests that 3 mM of ALT-711 has a potent duration of approximately 7 days but its effect is cumulative and can be continued by replenishing the solution. Based on the projection on the FL gradients in

Figure 7 and **Figure 8**, over 30 days of ALT-711 treatment may reverse a significant amount of FL gained by the glycation process.

iii) Undemineralized bone

Stability of pH over incubation period

Ribose-glycation solutions are known to become acidic over time [2, 3], which can lead to unwanted decalcification of bone specimens during a long incubation period. It is not known if ALT solutions exhibit similar behavior. In order to investigated whether ribose or ALT-711 solutions would maintain a neutral pH level (i.e. 7) over a 14 day incubation period at 37 °C, we prepared 25 ml solutions (**Table 4**) with combinations of PBS, ribose (666 mM), ALT-711 (3 mM) and $CaCl_2$ (57.5 mg/liter) [4].

There was only a minor decrease of pH level in ALT-711 solutions (**Table 4, Figure 9**). Unlike unbuffered saline solutions, addition of $CaCl_2$ to PBS solutions ALT resulted in a precipitate (potentially calcium phosphate), but this caused no discernible change to the pH. Based on these observations, we decided to use ALT solutions without additional buffers for the anticipated treatment durations. On the other hand, we found a marked decrease in pH (from 6.91 to 4.32) for all ribose solutions by the end of day 14 (**Table 4, Figure 9**), confirming the need to control pH in glycation solutions. By performing a daily titration of the solution with 0.1 M NaOH [2, 3], we were able to maintain the pH of the ribose solutions at 7.2 ± 0.4 (mean ± SD) throughout the 14 day period. Based on this result, we decided to continue with daily titration and weekly replenishment of the ribose solutions for the rest of the experiments.

Table 4. Description of the solutions and pH values over a 2 week period of incubation at 37 °C. The three ribose containing treatment groups (GLY, GLY+CaCl2, GLY+ALT) are substantially acidified in 14 days (marked by *) decreasing their pH from 7 to 4.32.

			pH measured		
Treatment group	n	Treatment solution	Day 0	Day 7	Day 14
Control	1	PBS	7.01	6.99	7.02
$CaCl_2$ control	1	PBS+$CaCl_2$	7.01	6.96	6.99
ALT	1	ALT-711+PBS	7.01	6.85	6.72
ALT+ $CaCl_2$	1	ALT-711+PBS+$CaCl_2$	7.01	6.87	6.74
GLY	2	Ribose+PBS	6.86	5.28	4.32*
GLY+ $CaCl_2$	1	Ribose+PBS+$CaCl_2$	6.82	5.42	4.35*
GLY+ALT	1	Ribose+ALT-711+PBS+$CaCl_2$	6.91	5.63	4.47*

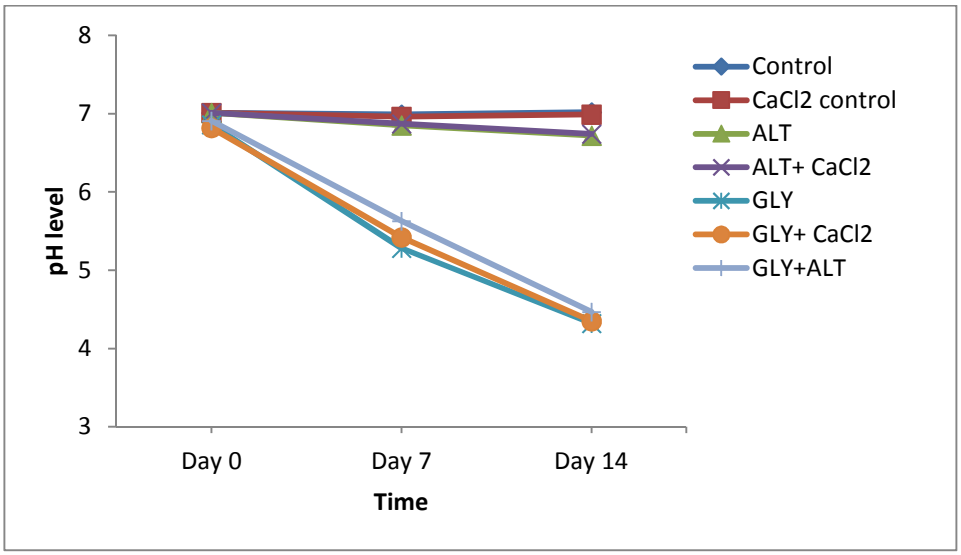

Figure 9: pH level change during a 14 day incubation period (37 °C) of ALT-711 (ALT) and ribose (GLY) solutions with and without $CaCl_2$. Any treatment solutions containing ribose (GLY) acidified quickly turning into a mild acid in two weeks.

In order to further refine and validate the dosage and duration of ALT treatment for undemineralized bone samples to be used in the mechanical tests, 2x2x5 mm beams (prepared from the region shown in **Figure 10**) were utilized. Beam dimensions were chosen to reflect the thickness of compact tension specimens (Task 3). Using a diamond circular saw (South Bay, San Diego), 36 beams were prepared from four donors (35 year old female, 50 year old male, 80 year old female and 81 year old male) representative of the gender and age groups of the main experiment.

The 36 beams were randomized and allocated into 3 x 4 wells (**Figure 10**), corresponding to three treatment groups (low ALT (3mM), high ALT (30mM) and control groups) and four time points (day 0, 7, 14, 21). All beams were initially subjected to a 2-week ribose glycation treatment (666 mM) at 37 °C. After the glycation treatment, ALT treated groups were subjected to 3 mM and 30 mM ALT solution for 7, 14 and 21 days (**Figure 5**) while the control was placed in a PBS solution.

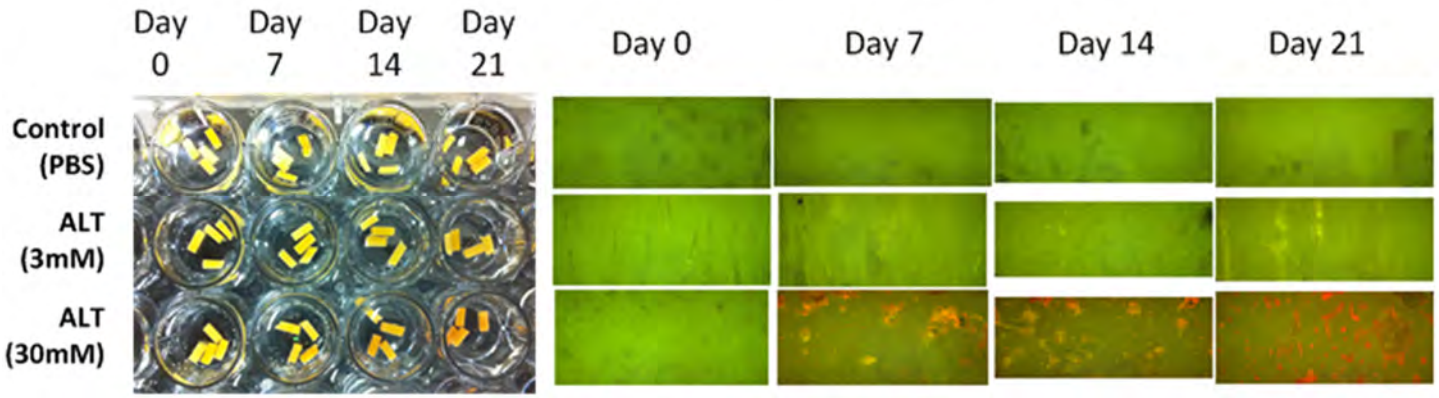

Figure 10: (Left) Bone beams allocated into 24-well plate in a 3 x 4 scheme representing three treatment groups (PBS, 3 mM and 30 mM ALT and four different time points from day 0 to day 21). (Right) Bone beams imaged using epi-fluorescence microscopy. The brightness of green fluorescence, a marker for glycation, decreased markedly with time in the 30 mM ALT group compared to the 3 mM ALT group and control, indicating ALT potentially reduces the amount of AGE crosslinks in the tissue.

The beams were processed similar to the methods of the bone powder experiment. The bone beams were first decalcified using 20% formic acid and then digested using papain solution (0.4 mg/mL in sodium acetate buffer) at 65°C for two days. The partially digested beams were crushed and further digested another two days without replacing the solution, and then specimens were centrifuged for 30 minutes at 11,000 rpm at 4 °C. 100 µl of the supernatant from each specimen was collected and analyzed using spectrophotometry. According to a two-way ANOVA, both the concentration and duration significantly affected the level of fluorescence ($p<0.003$ and $p<0.0001$, respectively); the level of fluorescence generally increased with concentration and duration of ALT

treatment. Post-hoc analyses using Tukey's test revealed that the significant effect of ALT (compared to PBS control) was observable at day 21 between the groups, but not before (**Figure 11**).

At this stage, the optimum concentration and duration of AGE-breaker solutions was determined for the next steps (Milestone 1).

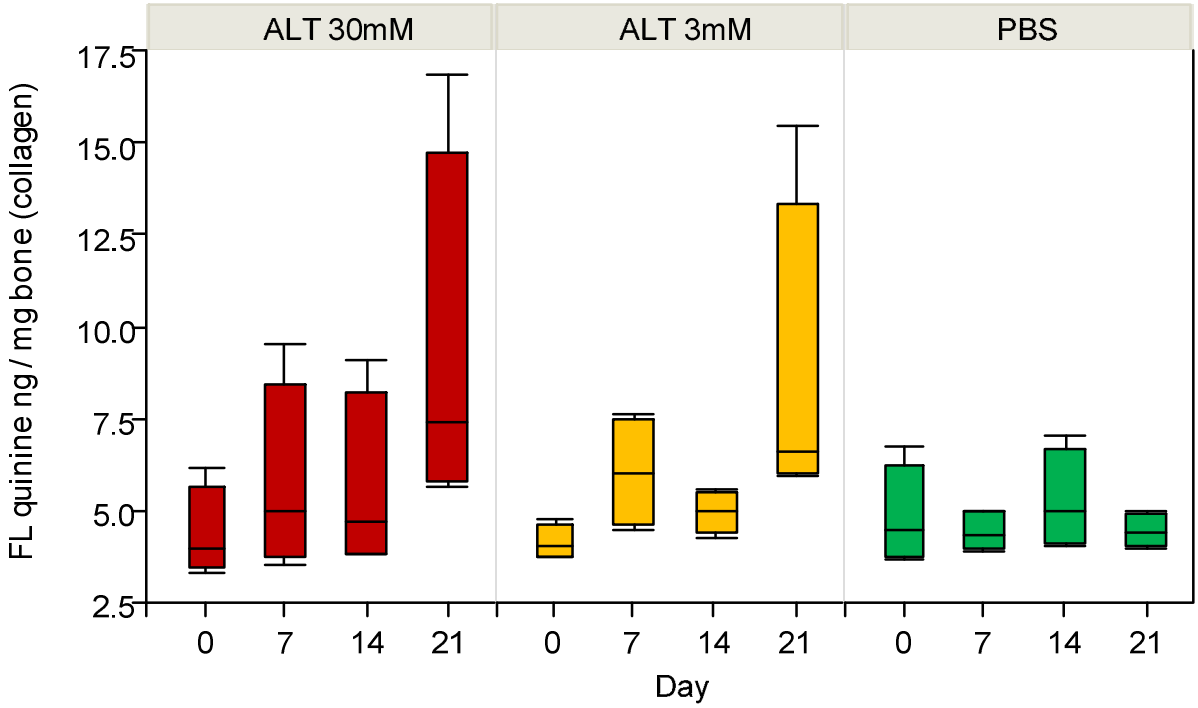

Figure 11: The amount of fluorescence under two ALT dosages (3 and 30 mM) over 21 days of treatment. An increase is observed in fluorescence level (FL) with increasing treatment duration for both 30 mM and 3 mM ALT dosages, with differences becoming significant at day 21. No change in FL was observed with increasing duration for the control (PBS).

Task 3. Preparation of test samples from 24 femurs. (Months 2-8.)

3a. Machining of 4 compact tension test specimens per femur using a CNC micromilling machine. (Months 2-6)
3b. Artificial glycation in ribose and AGE-breaker treatment of the normal and glycated subgroups (Months 7-8)

We have used a CNC milling machine (Denford Micromill 2000, West Yorkshire, UK) to machine compact tension (CT) specimens based on our previous work [5, 6]. While previous work used a saline drip irrigation method to prevent over heating of bone during machining, we machined the bone specimens submerged in a saline bath to further minimize the potential effects of heating and drying that may inadvertently degrade the bone quality (**Figure 12**).

Machining CT specimens fully submerged underwater required remanufacturing of the CNC machining station to incorporate a saline bath chamber, a mini vice and a drainage system. Furthermore, the CNC machining program was rewritten to account for special restrictions from machining underwater.

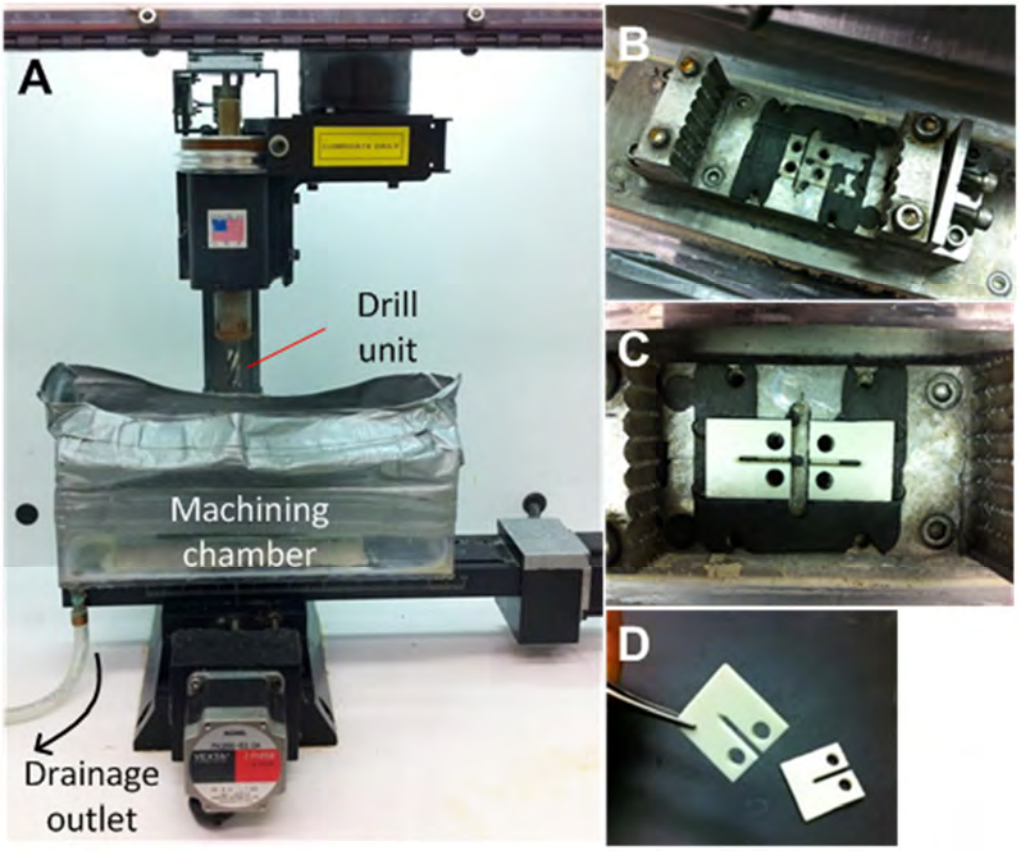

Figure 12: (A) CNC setup for compact tension (CT) specimen machining where the machining chamber was filled with saline during the entire machining process. The chamber contains (B) a specimen vice to grip the femoral section during the initial cutting process and (C) a die platform to hold the CT specimens during machining of the finer details. (D) Typical fully machined CT specimens.

From each femur, we sought to obtain as many samples as possible (**Figure 13**). 4 CT specimens were obtained from medial-proximal and lateral-proximal facets while the remaining bone was used to prepare 2x2 mm beams for complementary mechanical tests and 100-200 μm thick bone slices for Aim 2. We have processed 24 femurs in this manner obtaining 96 CT samples (24 donors x 4 treatments), which were scanned on a flatbed scanner to examine the symmetricity of the chevron notch. Using an image analysis software, tip-to-edge distances (**Figure 14**) were measured and used for calculating the offset distance of the notch tip from the center of the speciemen. The notch tip to center distance was 0.04 ± 0.39 mm (mean ± SD) for the whole group of 96 CT samples.

Following machining, all study specimens were treated according to their experimental group assignment (glycated, ALT-treated, both glycated and ALT-treated or untreated control. All mechanical test specimens were divided into four treatment groups and kept in PBS buffer together with chloroform (20 μL/25 mL) and gentamicin (25 μL/25 mL) to inhibit fungal and bacterial growth. GLY and GLY+ALT specimens were first incubated at 37 °C for two weeks in 666 mM ribose solution prepared with PBS, chloroform and gentamycin. The glycation solution was titrated daily with 0.1 M NaOH to maintain constant pH of 7.0. Following glycation, GLY+ALT specimens were incubated for another three weeks in 30 mM ALT-711 solution at 37°C. ALT specimens were not glycated but were incubated in 30 mM ALT-711 solution at 20 °C for three weeks. Control specimens received no treatment but were incubated at 20 °C for five weeks. All specimens were frozen at -20 °C following their respective treatments.

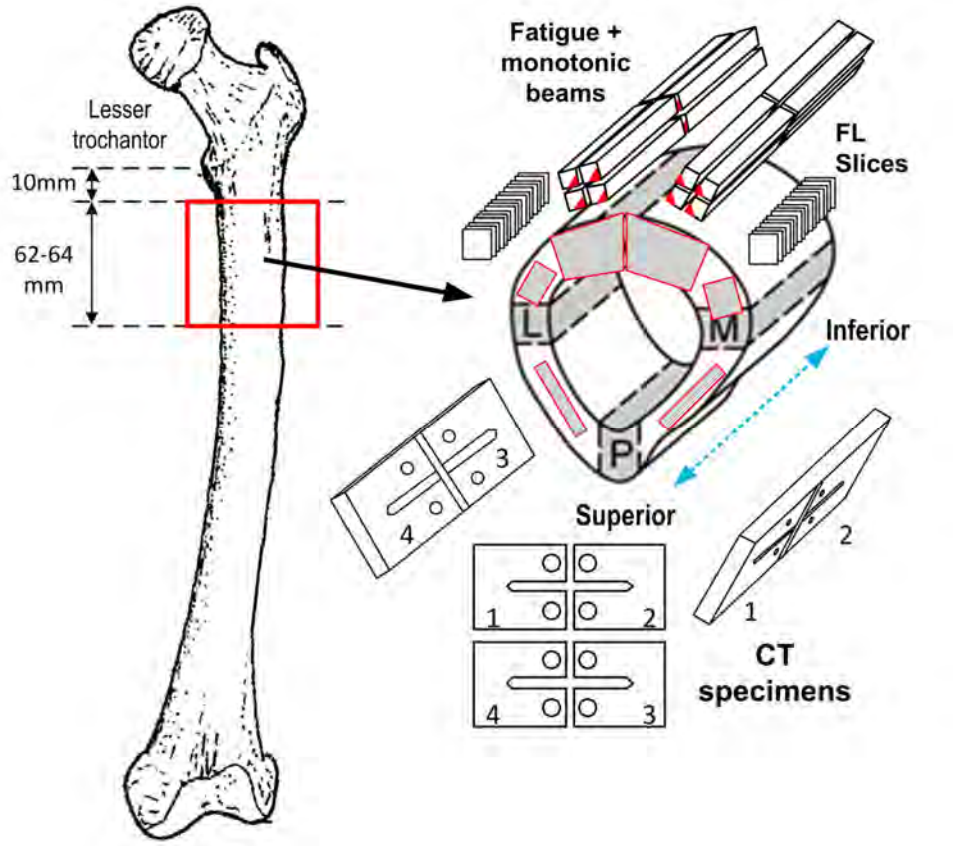

Figure 13: Cutting scheme of a femur. A 62-64 mm section was cut 10 mm below the lesser trochanter from each femur. The section was divided between medial and lateral segments and then CNC machined to produce four CT specimens from the postero-medial and postero-lateral cortices. The medial (M) and lateral (L) strips were used to cut 100 μm thick bone slices for the osteogenicity experiments. Additional rectangular beam specimens were machined from the antero-medial and antero-lateral cortices to be used in future fatigue and monotonic strength tests.

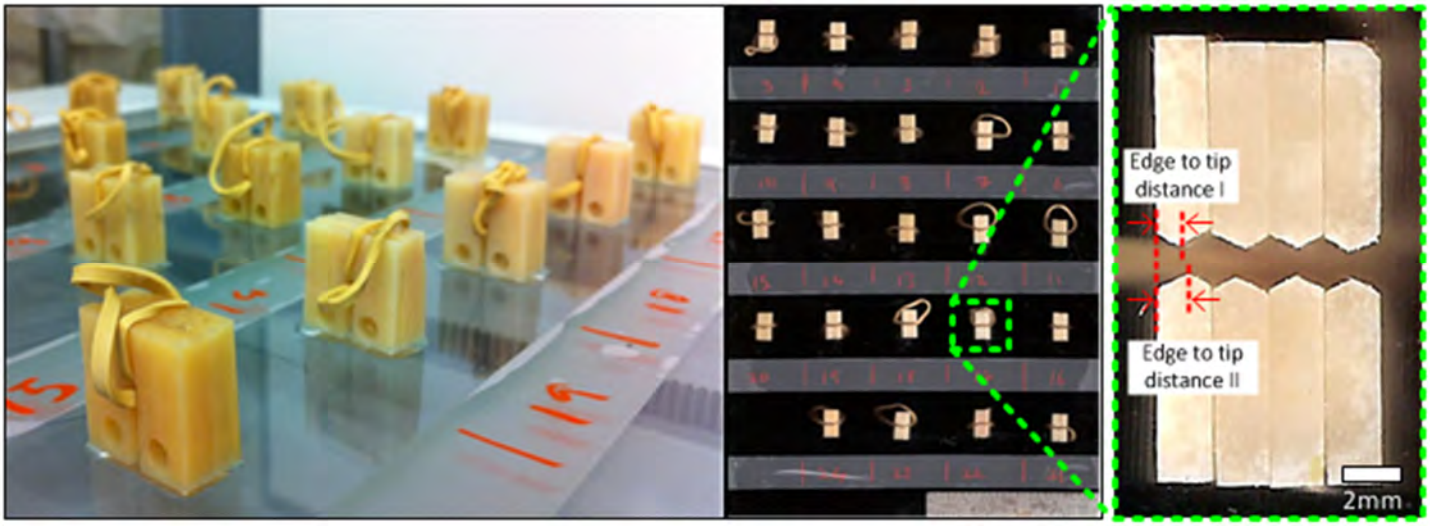

Figure 14: Four CT specimens from each donor were bound together by a rubber band and then scanned on a flatbed scanner to examine the chevron notch profile. Upper and lower edge-to-tip distances were measured and used to calculate the offset of each notch tip from the center of the specimen.

Task 4: Mechanical testing. (Months 19-23.)
4a. Fracturing the CT specimens using R-curve fracture toughness test methods. (Months 19-21.)
4b. Data reduction and calculation of fracture toughness. (Months 22-23.)

Refinement of R-curve test methods for measurement of crack resistance in bone specimens

In order to initiate controlled crack propagation, a pre-crack with 0.5 mm length was made at the tip of the chevron notch in the CT specimens by using a mechanical testing system (Biosyntech Mach 1) with a razor blade attachment (**Figure 15**). The precracking procedure incorporated a contact-load detection function to accurately define the initial point of contact between the edge of the razor blade and the notch tip. To optimize the cyclic loading parameters for the fracture toughness test in the same mechanical testing system (**Figure 16**), we used six extra CT specimens. After several trials, we found that a tensile displacement amplitude of 50 μm, followed by an immediate recovery of 30 μm at a rate of 5 μm/s provided more than six cycles of crack propagation prior to the sudden drop of tensile force, which allows for sufficient number of compliance calculations necessary for the construction of an R-curve. During the entire loading and unloading cycle, the sample was placed in an environmental chamber with constant saline irrigation.

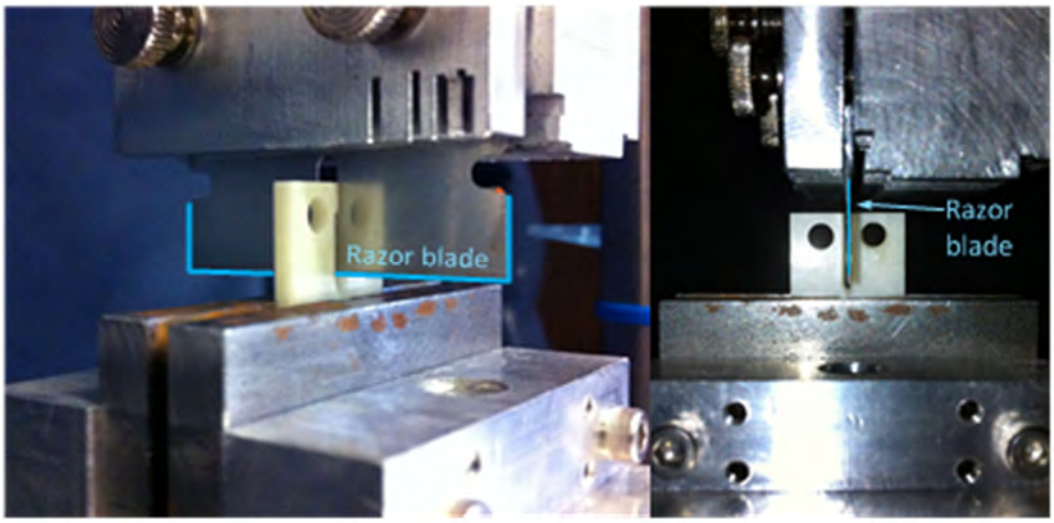

Figure 15: Prior to CT fracture toughness test, a pre-crack with a depth of 0.5mm was introduced at the tip of chevron notch using a razor blade (marked by the blue lines).

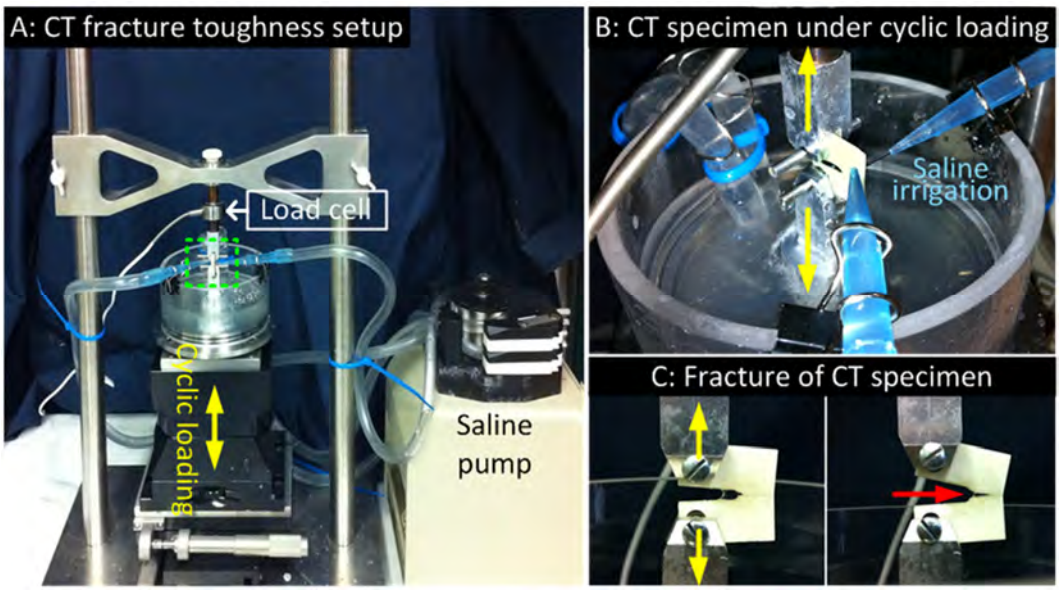

Figure 16: (A) CT specimen was cyclically loaded by a micromechanical tester with (B) constant saline irrigation. (C) Controlled propagation of a crack is achieved in the CT specimen (red arrow) upon continuous cyclic loading (yellow arrows). The purpose of the test is to determine the resistance of bone to the growth of this crack.

Fracture toughness (K_R) was calculated based on the following equation [7]:

$$K_R = \frac{PY(a/W)}{B\sqrt{W}}$$

where **P** is the maximum load associated with a crack advancement, **B** is specimen thickness, **W** is specimen width, **a** is crack length and **Y(a/W)** is a function of specimen geometry (**Figure 17**).

Following test protocol refinement, all study specimens that were treated according to their experimental group assignment (glycated, ALT-treated, both glycated and ALT-treated or untreated control), were tested to determine their R-curve behavior.

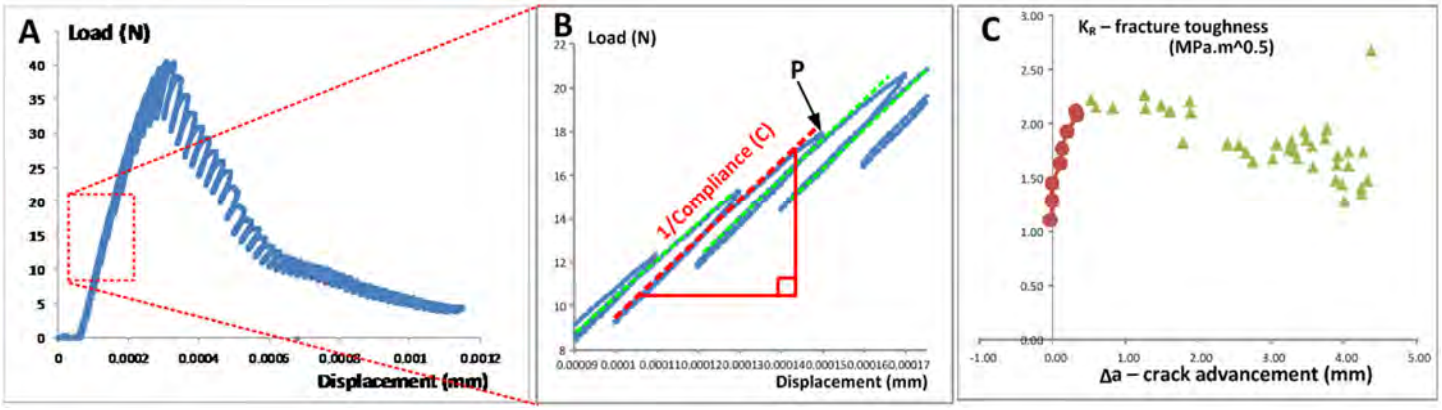

Figure 17: (A) Load-displacement curve from a typical R-curve test conducted on a bone specimen, showing series of loading-unloading cycles. (B) For each loading-unloading cycle, C (compliance) and P (maximum load) are measured. The series of compliance values are used to calculate a series of crack length values. (C) The load and crack length data are then used to construct an R-curve where fracture toughness (K_R) is plot as a function of increases in crack length (Δa) [7-9]. The rising portion of the R-curve (red) represents increasing resistance to crack propagation whereas the falling portion (green) signifies a decline in the resistance.

From the measured R-curves, the following outcome variables were calculated for each specimen:
K_0: Crack initiation fracture toughness. Calculated as the K_R at the beginning of the R-curve, the first point at which a compliance change was observed during the load-unload cycles.
K_{max}: Peak stress intensity factor. Calculated as the peak K_R value on the R-curve, the point at which stable crack growth ends and unstable crack growth begins.
Δa_{max}: Maximum crack length. The crack length value corresponding to K_{max}. Indicates how big the crack can grow before it becomes unstable.
R: Overall crack resistance. Calculated as the slope of the log-transformed R-curve (Log-K vs Log-Δa) from a=0 to a=a_{max}).

Specimen geometry variables were measured for quality control purposes (Figure 18):
B: Specimen thickness: Measured from the digitized images of the specimen surface. The average value of specimen thickness (2.02 mm) was very close to the desired value (2.00 mm) with a small variation (StDev = ±0.03 mm).
n_e: Notch eccentricity: The offset of the notch tip from the center of the specimen. This was measured for both sides of the notch using the digitized images of the specimen and an average was recorded. The values of notch eccentricity were small but (0.04±0.03 mm).
n_a: Notch asymmetry: The distance between the two sides of the notch tip. The values of notch asymmetry were small but (0.16±0.17 mm).

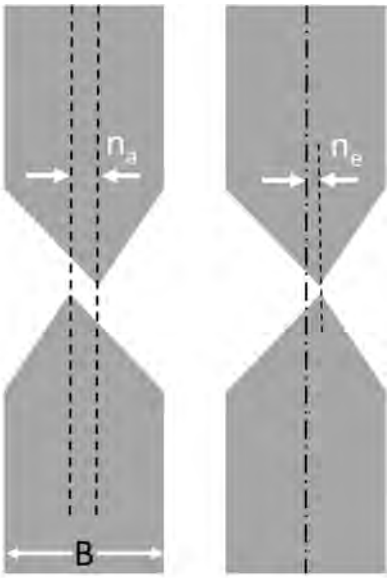

Figure 18: Specimen thickness (B), notch asymmetry (n_a) and notch eccentricity (n_e). The eccentricity and asymmetry are exaggerated for the purpose of illustration.

At this stage, the effect of AGE-breakers on the R-curve fracture toughness of cortical bone is determined (Milestone 2).

Table 5. Descriptive data for variables measured from R-curve tests in Task 4. Average ± standard deviation is reported for each variable.

ALT	Old Male	Old Female	Young Male	Young Female	Male	Female
K_0 (MPa.mm$^{1/2}$)	1.204 ± 0.137	1.165 ± 0.276	1.226 ± 0.204	1.315 ± 0.150	1.215 ± 0.166	1.240 ± 0.226
Δa_{max} (mm)	0.384 ± 0.297	1.037 ± 0.644	0.601 ± 0.313	0.662 ± 0.485	0.493 ± 0.312	0.850 ± 0.578
K_{max} (MPa.mm$^{1/2}$)	1.495 ± 0.267	1.735 ± 0.227	1.643 ± 0.310	1.789 ± 0.169	1.569 ± 0.286	1.762 ± 0.193
R (MPa.mm$^{-1/2}$)	0.071 ± 0.027	0.086 ± 0.026	0.056 ± 0.030	0.076 ± 0.020	0.063 ± 0.028	0.081 ± 0.023
	Old		Young		Pooled	
K_0 (MPa.mm$^{1/2}$)	1.184 ± 0.209		1.271 ± 0.177		1.228 ± 0.194	
Δa_{max} (mm)	0.711 ± 0.587		0.631 ± 0.39		0.671 ± 0.489	
K_{max} (MPa.mm$^{1/2}$)	1.615 ± 0.267		1.716 ± 0.25		1.665 ± 0.258	
R (MPa.mm$^{-1/2}$)	0.079 ± 0.026		0.066 ± 0.026		0.072 ± 0.026	

CONTROL	Old Male	Old Female	Young Male	Young Female	Male	Female
K_0 (MPa.mm$^{1/2}$)	1.119 ± 0.290	1.302 ± 0.096	1.280 ± 0.159	1.264 ± 0.131	1.199 ± 0.238	1.283 ± 0.111
Δa_{max} (mm)	0.632 ± 0.065	0.441 ± 0.233	0.514 ± 0.337	0.634 ± 0.229	0.573 ± 0.239	0.538 ± 0.242
K_{max} (MPa.mm$^{1/2}$)	1.517 ± 0.325	1.876 ± 0.314	1.623 ± 0.241	1.860 ± 0.471	1.570 ± 0.278	1.868 ± 0.382
R (MPa.mm$^{-1/2}$)	0.077 ± 0.032	0.077 ± 0.02	0.064 ± 0.025	0.090 ± 0.066	0.071 ± 0.028	0.084 ± 0.047
	Old		Young		Pooled	
K_0 (MPa.mm$^{1/2}$)	1.211 ± 0.227		1.272 ± 0.139		1.241 ± 0.187	
Δa_{max} (mm)	0.536 ± 0.191		0.574 ± 0.282		0.555 ± 0.236	
K_{max} (MPa.mm$^{1/2}$)	1.697 ± 0.358		1.742 ± 0.378		1.719 ± 0.361	
R (MPa.mm$^{-1/2}$)	0.077 ± 0.026		0.077 ± 0.049		0.077 ± 0.038	

GLY	Old Male	Old Female	Young Male	Young Female	Male	Female
K_0 (MPa.mm$^{1/2}$)	1.182 ± 0.165	1.256 ± 0.264	1.433 ± 0.063	1.429 ± 0.163	1.307 ± 0.177	1.342 ± 0.228
Δa_{max} (mm)	0.538 ± 0.384	0.712 ± 0.45	0.517 ± 0.197	0.382 ± 0.159	0.527 ± 0.291	0.547 ± 0.365
K_{max} (MPa.mm$^{1/2}$)	1.756 ± 0.228	1.737 ± 0.309	1.889 ± 0.161	1.909 ± 0.191	1.823 ± 0.201	1.823 ± 0.261
R (MPa.mm$^{-1/2}$)	0.103 ± 0.030	0.080 ± 0.051	0.064 ± 0.025	0.092 ± 0.021	0.084 ± 0.033	0.086 ± 0.038
	Old		Young		Pooled	
K_0 (MPa.mm$^{1/2}$)	1.219 ± 0.213		1.431 ± 0.118		1.325 ± 0.200	
Δa_{max} (mm)	0.625 ± 0.409		0.450 ± 0.184		0.537 ± 0.323	
K_{max} (MPa.mm$^{1/2}$)	1.747 ± 0.259		1.899 ± 0.169		1.823 ± 0.228	
R (MPa.mm$^{-1/2}$)	0.091 ± 0.042		0.078 ± 0.027		0.085 ± 0.035	

GLY+ALT	Old Male	Old Female	Young Male	Young Female	Male	Female
K_0 (MPa.mm$^{1/2}$)	1.187 ± 0.242	1.267 ± 0.303	1.198 ± 0.133	1.392 ± 0.274	1.193 ± 0.186	1.336 ± 0.28
Δa_{max} (mm)	0.820 ± 0.209	0.736 ± 0.321	0.802 ± 0.202	0.633 ± 0.314	0.811 ± 0.196	0.680 ± 0.306
K_{max} (MPa.mm$^{1/2}$)	1.627 ± 0.157	1.751 ± 0.431	1.816 ± 0.302	1.955 ± 0.388	1.722 ± 0.25	1.862 ± 0.401
R (MPa.mm$^{-1/2}$)	0.078 ± 0.033	0.073 ± 0.019	0.101 ± 0.040	0.089 ± 0.034	0.089 ± 0.037	0.082 ± 0.028
	Old		Young		Pooled	
K_0 (MPa.mm$^{1/2}$)	1.224 ± 0.26		1.295 ± 0.229		1.261 ± 0.242	
Δa_{max} (mm)	0.782 ± 0.255		0.717 ± 0.267		0.748 ± 0.257	
K_{max} (MPa.mm$^{1/2}$)	1.683 ± 0.301		1.886 ± 0.339		1.789 ± 0.331	
R (MPa.mm$^{-1/2}$)	0.076 ± 0.026		0.095 ± 0.036		0.086 ± 0.033	

Task 5. Preparation of bone substrates for cell cultures from 24 femurs. (Months 19-22.)

5a. Preparation of 100 µm-thick sections (triplicates per measurement) from the middiaphysis. (Months 4-5.)

5b. Demineralization of bone sections in EDTA solutions. (Months 5-6.)

5c. Artificial glycation in ribose and AGE-breaker treatment of the normal and glycated subgroups. (Months 6-7.)

5d. Culture human mesenchymal stem cells (Lonza, Walkersville, MD) on bone sections. (Months 19-24.)

While machining CT and beam specimens from each femur for Aim 1, we also prepared approximately 500 100-200 μm thick bone slices (**Figure 13**) under this task. Bone substrate specimens were demineralized for two days in 0.1 M EDTA. Following demineralization, specimens were cut to a uniform size using a 6mm diameter biopsy punch (**Figure 19**). The bone substrate specimens were divided into four groups (Glycation, Glycation + ALT, ALT and control). Specimens allocated to the Glycation and Glycation + ALT groups were treated for one week under glycation (666 mM ribose). Specimens allocated to ALT and Glycation + ALT groups were treated for two weeks under ALT (30mM ALT-711). Control specimens were kept untreated.

Following their respective treatments, the bone sections were used as substrates for human stem cells (Lonza, Walkersville, MD). Prior to cell culture, the bone sections were washed with ethanol, hood-dried for 30 minutes and then washed again using PBS. The sections were kept in 10% bovine fetal serum DMEM solution mix with Fungizone overnight.

The bone sections were placed in 6 well culture plates, seeded with the stem cells and cultured under conditions shown to induce osteogenic differentiation (minimal essential medium supplemented with 10% fetal calf serum, 0.1 μM dexamethasone, 10 nM β-glycerol phosphate, and 50 μg/ml ascorbic acid phosphate). For PCR experiments (Task 9), cell culture was terminated at two time points (7 and 14 days) to assess gene expression as a function of cell culture duration. For tasks 6/7 (cell division and apoptosis) and 8 (mineralization), cell culture was terminated at 21 days in order to assess bone substrates at later stages of osteogenic differentiation.

Figure 19: Approximately 500 bone slices of 6 mm diameter (by using a 6mm diameter biopsy punch) were obtained from 24 femurs and divided into four treatment groups (Glycation, Glycation + ALT-711, ALT-711 and control).

Task 6. Measure incorporation of ethynyl deoxyuridine using fluorescent microscopy, express as the percentage of the population of cells undergoing cell division. (Months 24-25.)
Task 7. Tunel-stain and measure apoptotic cell density using fluorescent microscopy. (Months 25-26.)

Tasks 6 and 7 (ethynyl deoxyuridine and Tunel staining) were combined per CDMRP approval in communication dated 11/21/2014. There are extensive context- and tissue dependent limitation and artifacts using the TUNEL stain [10, 11] and we expected this to be compounded by challenges staining cells grown on bone slices. In addition, we observed substantial variability in the number of cells that attached to the bone slices. By substituting propidium iodide (PI) staining for the TUNEL technique, we were able to avoid the limitations of this technique and employed a method that provided an accurate measure of the number of cells on each bone slice in addition to the proportion of cells undergoing apoptosis. PI staining allowed the relative quantification and assessment of the morphology and spatial distribution of bone normal and apoptotic cells that could not be provided by TUNEL staining[12].

Following cell culture, specimens were prepared and stained for quantification of cell division using the Alexa

Fluor 594 Click-iT EdU Imaging Kit as described by the manufacturer (Invitrogen, Life Technologies, Carlsbad, CA). Briefly, bone slices were incubated with EdU labeling solution for 4 h. Cells were fixed with formaldehyde, washed in PBS and EdU detected after Triton-X100 permeabilization using the Click-iT reaction cocktail. Bone slices were counter stained for quantification of cell number and detection of apoptosis by incubation with Hoechst 33342 for 30 min. Following staining, specimens were removed from well plates and mounted on microscope slides using aqueous mounting medium. For each of four treatment groups (GLY+ALT, ALT, GLY, and Control), a total of 48 100-200 µm thick bone slice specimens (**Figure 13**) – 3 specimens from each of 4 age/gender groups (old/young female/male) – were used in this task.

Microscope images were obtained from each bone slice (Nikon Corp., Tokyo, Japan) using a 10x objective and 590 nm fluorescence excitation for EdU (Alexa Fluor 594) and 350 nm fluorescence excitation for Hoechst 33342 nuclear staining. Bone slices were imaged at four random locations and measurements were averaged in order to provide a quantity representative of the entire bone slice. Manual cell counting was facilitated using a grid overlay on each image using imageJ [13]. Total number of viable cells (#Live) and apoptotic cells (#Apoptotic) was quantified from the Hoechst nuclear stained images, and total number of dividing (#Dividing) cells was quantified from the EdU stained images (Figure 20). Percentage of dividing cells (%Div) was calculated as 100*(#Dividing/#Live) (Figure 21). Percentage of apoptotic cells (%Apop) was calculated as 100*(#Apoptotic/#Live) (Figure 22).

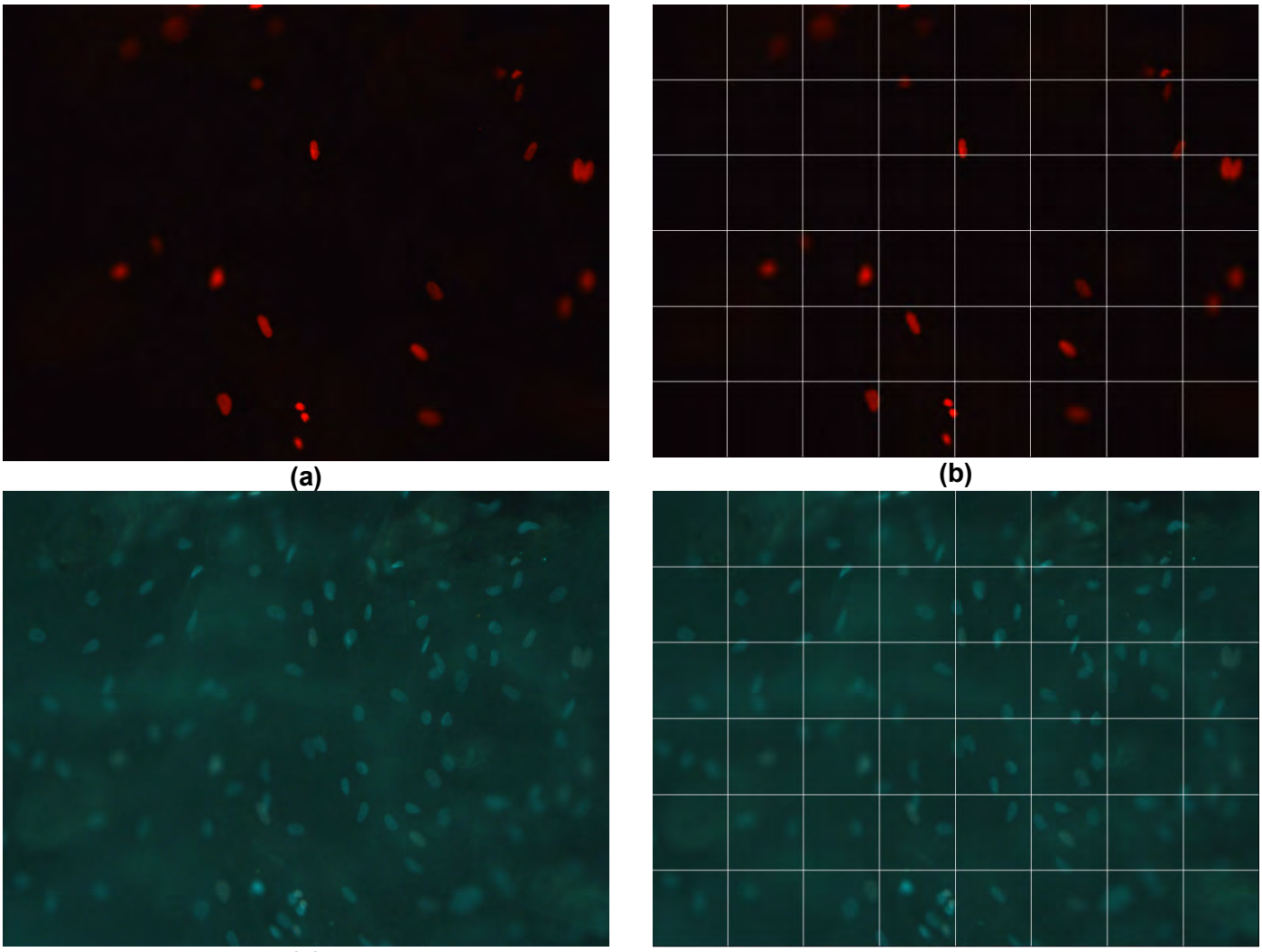

Figure 20: Prepared bone slices were stained for detection of cell division via ethynyl deoxyuridine (a) and cell viability and apoptosis via Hoechst nuclear staining (c). Grids were overlaid on each image to facilitate manual cell counting, from which percentage of dividing and apoptotic cells was derived (b and d).

Table 6. Cell division and apoptosis as measured from EdU and Hoechst stained images in Task 6/7. Average ± standard deviation is reported for each variable.

ALT	Old Male	Old Female	Young Male	Young Female	Male	Female
%Div	18 ± 12.4	31.4 ± 30.6	22.8 ± 19.1	13.4 ± 10.9	20.4 ± 14.7	22.4 ± 22.8
%Apop	2 ± 2.5	2.4 ± 1.7	3.8 ± 3.3	0.7 ± 0	2.9 ± 2.8	1.5 ± 1.4
	Old		Young		Pooled	
%Div	24.7 ± 22.1		18.1 ± 14.9		21.4 ± 18.3	
%Apop	2.2 ± 1.9		2.3 ± 2.7		2.2 ± 2.2	

CONTROL	Old Male	Old Female	Young Male	Young Female	Male	Female
%Div	14.6 ± 9.1	34.1 ± 9.8	14.1 ± 11	29 ± 4.8	14.3 ± 9	31.5 ± 7.5
%Apop	0.9 ± 0.8	1.5 ± 0.7	1.1 ± 1	0.7 ± 0.2	1 ± 0.8	1.1 ± 0.6
	Old		Young		Pooled	
%Div	24.4 ± 13.7		21.5 ± 11.1		22.9 ± 12	
%Apop	1.2 ± 0.7		0.9 ± 0.7		1 ± 0.7	

GLY	Old Male	Old Female	Young Male	Young Female	Male	Female
%Div	11.5 ± 2.4	8.3 ± 2.8	19.4 ± 10.2	10.4 ± 11.2	15.5 ± 7.9	9.4 ± 7.4
%Apop	0.9 ± 0.9	2.7 ± 1.7	5.2 ± 5.6	5.5 ± 4.1	3.1 ± 4.3	4.1 ± 3.2
	Old		Young		Pooled	
%Div	9.9 ± 2.9		14.9 ± 10.8		12.4 ± 8	
%Apop	1.8 ± 1.6		5.4 ± 4.4		3.6 ± 3.7	

GLY+ALT	Old Male	Old Female	Young Male	Young Female	Male	Female
%Div	17.8 ± 18.2	7.5 ± 2.8	14.9 ± 8.5	12.2 ± 1.6	16.6 ± 13.7	9.9 ± 3.3
%Apop	5.4 ± 8.8	1.6 ± 1.5	1.4 ± 0.4	1.4 ± 1.1	3.8 ± 6.6	1.5 ± 1.1
	Old		Young		Pooled	
%Div	12.6 ± 13		13.3 ± 4.6		12.9 ± 9.6	
%Apop	3.5 ± 6		1.4 ± 0.8		2.6 ± 4.4	

At this stage, the effect of AGE-breakers on cell division and apoptosis determined (Milestones 3 and 4).

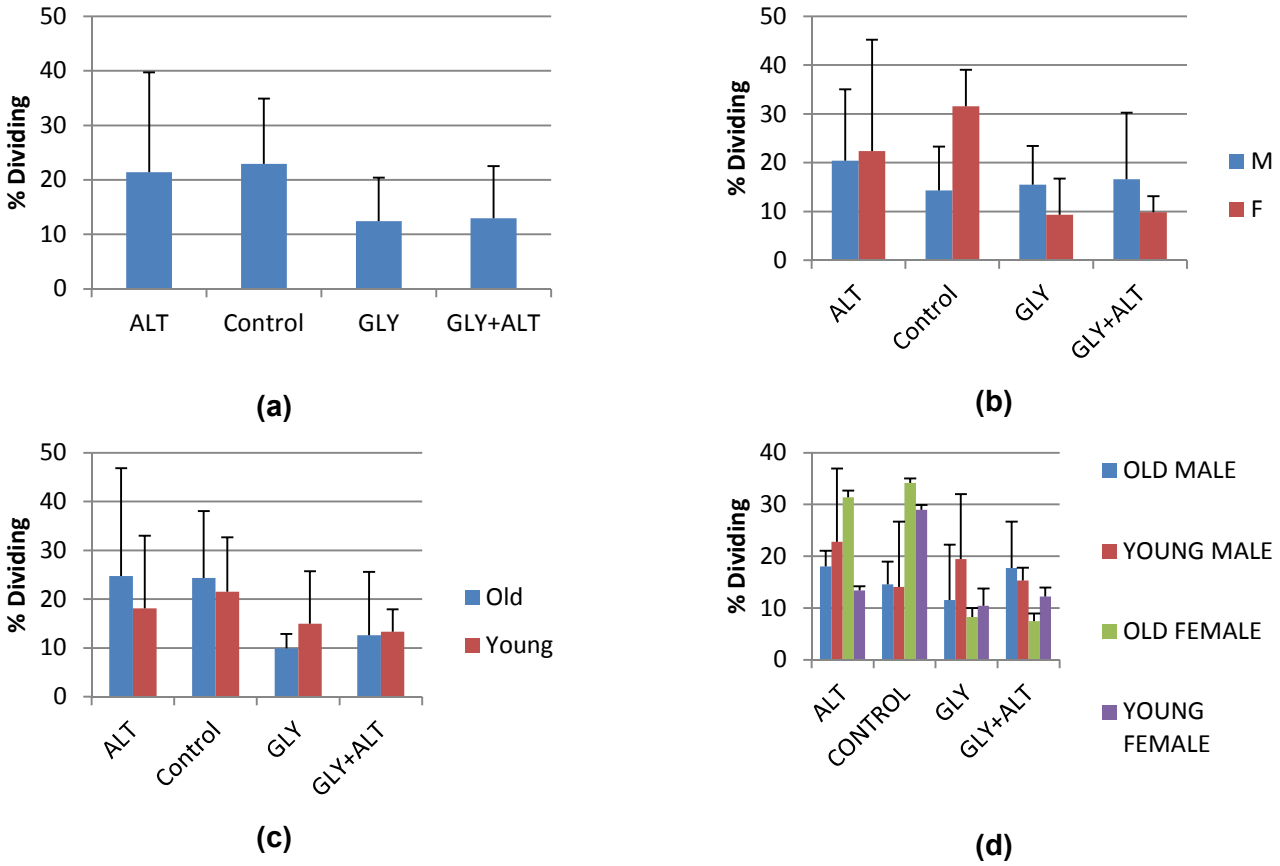

Figure 21: Percentage of dividing cells (%Div) as assessed by EdU staining, pooled (a) and separated by gender (b), age (c), and age-gender (d). Error bars indicate standard deviation.

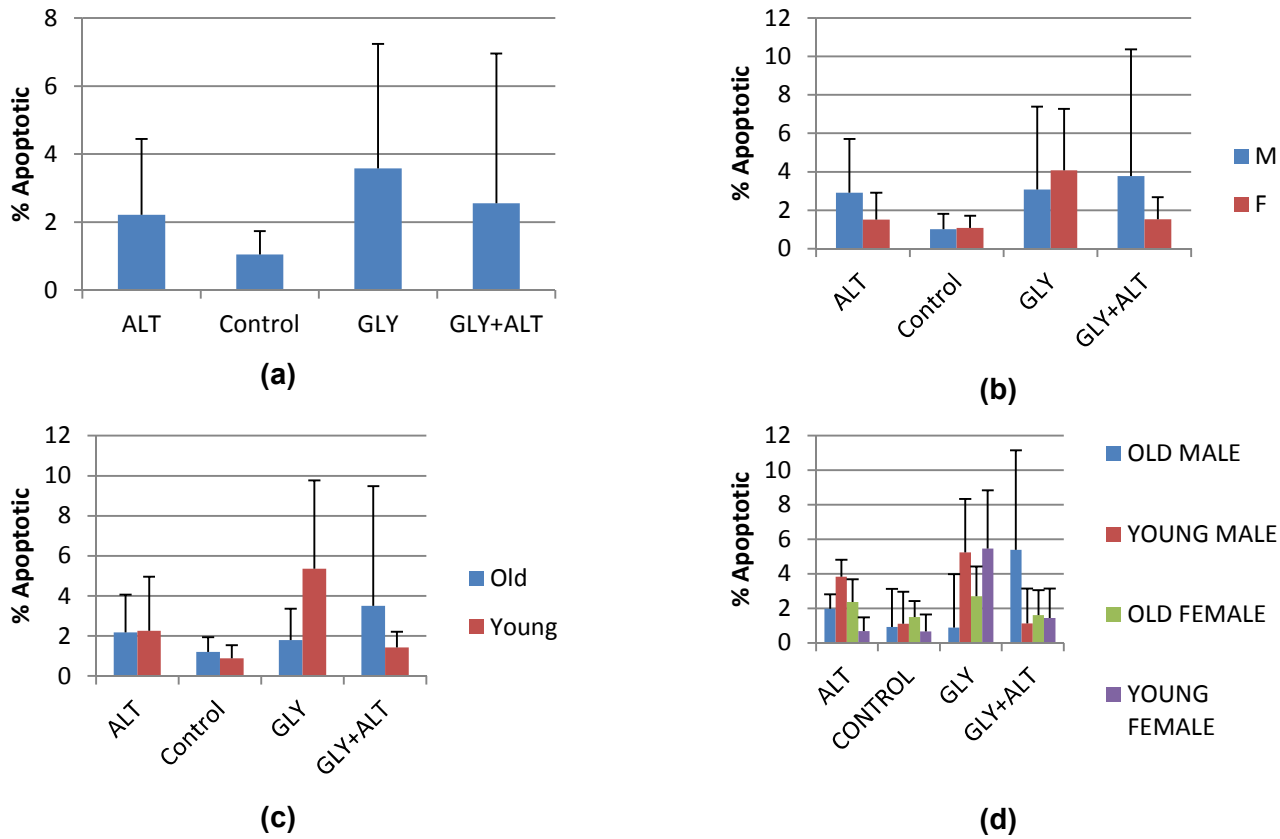

Figure 22: Percentage of apoptotic cells (%Apop) as assessed by Hoechst nuclear staining, pooled (a) and separated by gender (b), age (c), and age-gender (d). Error bars indicate standard deviation.

Task 8. Measure mineral nodules using the Von Kossa stain or histochemical detection of alkaline phosphatase. (Months 26-27.)

Following cell culture, specimens were prepared and stained for quantification of mineralization using alizarin red. Following staining, specimens were removed from well plates and placed on microscope slides with coverslips and mounted using aqueous mounting medium. Microscope images were obtained from each bone slice (Nikon Corp., Tokyo, Japan) using a 4x objective and white light. For each of four treatment groups (GLY+ALT, ALT, GLY, and Control), a total of 48 100-200 μm thick bone slices (Figure 13) – 3 specimens from each of 4 age/gender groups (old/young female/male) – were used in this task.

Mineralization was quantified as the red-positive area per total area. Microscope images were decomposed into their composite red, green, and blue channels. A single threshold value was determined for the 48 bone slice images by evaluating the red-channel images together as a single stack via the method of moments. The threshold value was then applied to each image individually (Figure 23). Percent mineralized area (%Min.Ar) was calculated as 100*(RedPositiveArea/TotalArea) (Table 7, Figure 24).

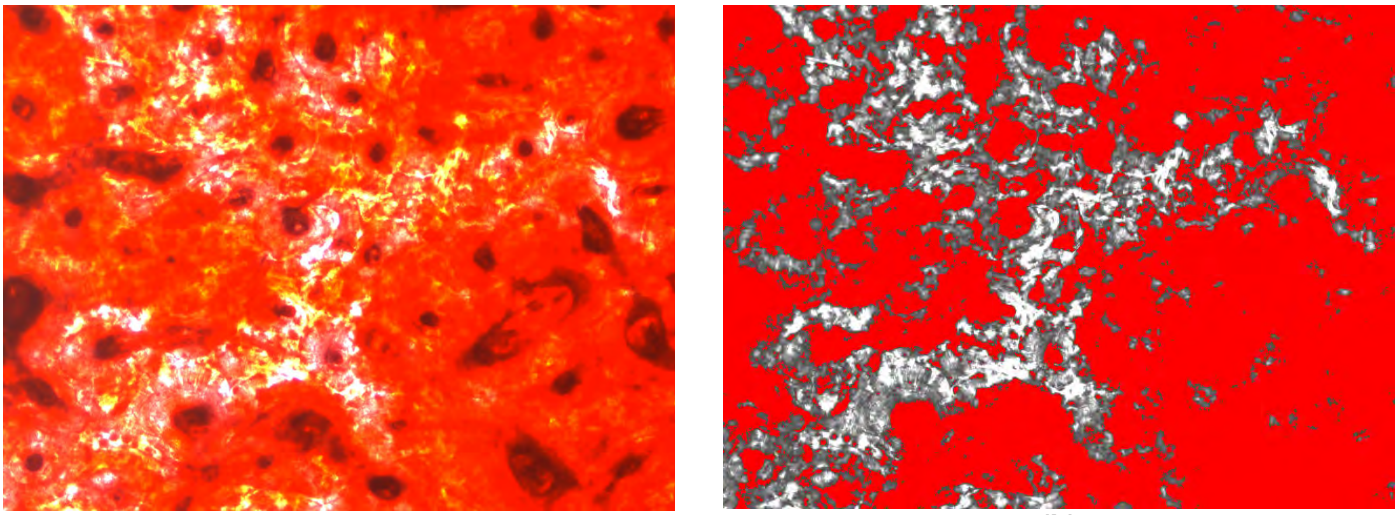

(a) **(b)**

Figure 23: Prepared bone slices were stained for mineral content using alizarin red (a). Alizarin-stained images were thresholded to quantify percent mineralized area (b).

Table 7. Mineralization measured as the percentage of mineralized areas from Alizarin stained images in Task 8. Average ± standard deviation is reported for each variable.

ALT	Old Male	Old Female	Young Male	Young Female	Male	Female
%Min.Ar	99.1 ± 1.2	98.4 ± 2.4	99.5 ± 0.6	96.7 ± 2.4	99.3 ± 0.8	97.5 ± 2.3
	Old		Young		Pooled	
%Min.Ar	98.7 ± 1.7		98.1 ± 2.2		98.4 ± 1.9	

CONTROL	Old Male	Old Female	Young Male	Young Female	Male	Female
%Min.Ar	92.7 ± 9.2	99.7 ± 0.2	93.9 ± 6.7	99.3 ± 1	93.3 ± 7.3	99.5 ± 0.7
	Old		Young		Pooled	
%Min.Ar	96.2 ± 7		96.6 ± 5.2		96.4 ± 5.9	

GLY	Old Male	Old Female	Young Male	Young Female	Male	Female
%Min.Ar	97.1 ± 3.4	95.9 ± 3.4	93.7 ± 7.7	85.1 ± 16.4	95.4 ± 5.6	90.5 ± 12.1
	Old		Young		Pooled	
%Min.Ar	96.5 ± 3.1		89.4 ± 12.4		92.9 ± 9.4	

GLY+ALT	Old Male	Old Female	Young Male	Young Female	Male	Female
%Min.Ar	95.1 ± 7.4	91.5 ± 7.5	84.7 ± 5.3	98.2 ± 2.4	89.9 ± 8.1	94.9 ± 6.2
	Old		Young		Pooled	
%Min.Ar	93.3 ± 6.9		91.4 ± 8.3		92.4 ± 7.4	

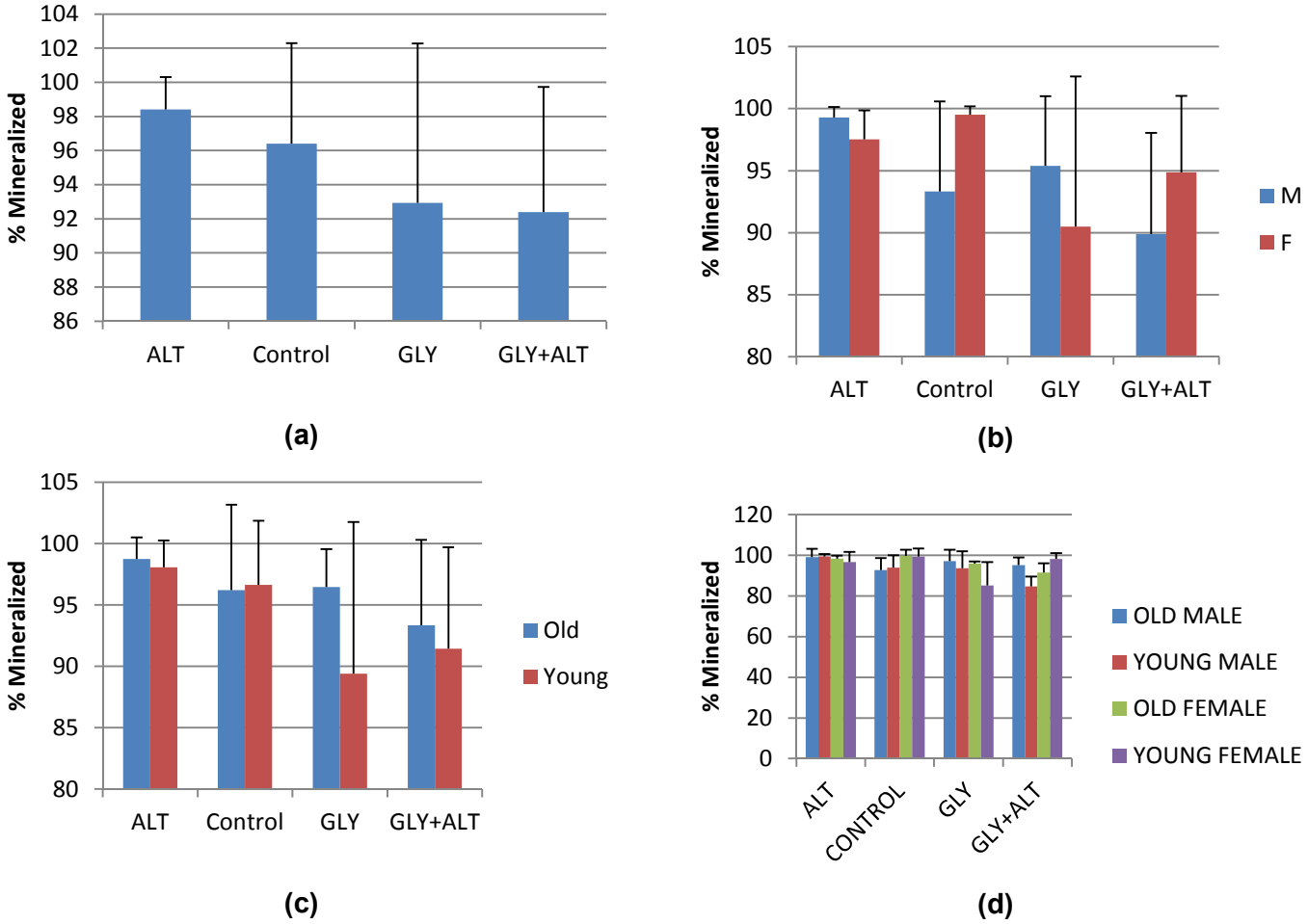

Figure 24: Percentage mineralized area (%Min.Ar) as assessed by Alizarin staining, pooled (a) and separated by gender (b), age (c), and age-gender (d). Error bars indicate standard deviation.

Task 9. Measure expression of molecular markers of mineralization, osteocalcin, RUNX2 and COL1A1 using quantitative RT-PCR with specific primers. (Months 28-29.)

RT-PCR was performed in duplicate using the TaqMan qPCR assay. Each PCR application reaction was performed in a final volume of 20 μl containing 1.2 μl of cDNA, 10 μl TaqMan 2x universal PCR Master mix, 1 μl of the specific primer/probe mix, and 7.8 μl of pure water. RT-PCR was carried out on an Applied Biosystems 7500 thermocycler, using the following condition: 95°C for 10 min, followed by 40 cycles of 95°C for 15 s and 60 °C for 1 min. Raw data was analysed with SDS relative Quantification Software version 2.2.3 (Applied Biosystems, Inc). We have measured four gene expression markers (**Table 8**) that indicate the activity and stage of cell differentiation and then compared with the known temporal gene expression patterns from the literature. And then using those relative levels of gene expression markers, we statistically compared between four groups at day 7 and 14.

Table 8. Summary of osteogenic markers used in this study.

Osteogenic marker	**Description**
Alkaline phosphatase (ALPH)	Associated with early cellular activity and differentiation but not bone specific
Collagen, type I, alpha 1 (COL1A1)	Associated with cell adhesion, proliferation and differentiation of the osteoblast phenotype and known as an early indicator of osteoblastic differentiation
RUNX2 (RUNX2)	Associated with osteoblastic differentiation and skeletal development
Osteocalcin (OCN)	Osteoblast specific protein, used as a marker for bone formation process (matrix synthesis and mineralization)

Table 9. RT-PCR results (mean and standard deviation) after 7 and 14 day culture showing expression levels relative to internal control (ΔCT), relative to control substrates in PBS (untreated bone; (ΔΔCT-PBS) and relative to cells on plastic substrate (no bone substrate; (ΔΔCT-no substrate) at day 7 and 14 respectively. Osteocalcin was not measured at day 7 because it is not expected to be expressed at early stages of differentiation. Note that all Δ and ΔΔ variables were calculated such that increasing values correspond to increasing expression. Fold increases can be calculated using the form $2^{\Delta\Delta CT}$.

ΔCT		ALT		GLY		GLY+ALT		CONTROL	
		Day 7	Day 14	Day 7	Day 14	Day 7	Day 14	Day 7	Day 14
ALPH	Mean	-7.49	-6.49	-6.42	-5.71	-6.59	-5.82	-7.26	-7.03
	SD	0.29	0.38	0.06	0.17	0.14	0.32	0.48	0.42
COL1A1	Mean	1.04	0.83	0.10	0.18	-0.19	0.34	0.67	1.12
	SD	0.42	0.27	0.24	0.52	0.35	0.21	0.50	0.61
RUNX2	Mean	-8.05	-7.92	-8.20	-7.38	-8.31	-7.65	-8.20	-7.86
	SD	0.19	0.31	0.07	0.27	0.22	0.25	0.26	0.50
OCN	Mean	-	-14.02	-	-13.33	-	-13.67	-	-13.42
	SD	-	1.21	-	0.26	-	0.63	-	0.74

ΔΔCT-PBS		ALT		GLY		GLY+ALT		CONTROL	
		Day 7	Day 14	Day 7	Day 14	Day 7	Day 14	Day 7	Day 14
ALPH	Mean	0.86	1.48	1.78	2.50	1.59	2.36	1.04	1.03
	SD	0.17	0.35	0.07	0.29	0.16	0.56	0.29	0.30
COL1A1	Mean	1.33	0.82	0.68	0.55	0.56	0.58	1.05	1.06
	SD	0.40	0.16	0.11	0.23	0.14	0.09	0.40	0.35
RUNX2	Mean	1.11	0.97	1.00	1.42	0.93	1.17	1.01	1.04
	SD	0.15	0.21	0.05	0.28	0.14	0.22	0.18	0.31
OCN	Mean	-	0.83	-	1.08	-	0.91	-	1.12
	SD	-	0.57	-	0.21	-	0.43	-	0.65

ΔΔCT-no substrate		ALT		GLY		GLY+ALT		CONTROL	
		Day 7	Day 14	Day 7	Day 14	Day 7	Day 14	Day 7	Day 14
ALPH	Mean	1.31	2.81	2.71	4.73	2.42	4.46	1.58	1.95
	SD	0.26	0.66	0.11	0.55	0.24	1.05	0.45	0.56
COL1A1	Mean	1.02	4.09	0.52	2.73	0.43	2.90	0.80	5.26
	SD	0.31	0.77	0.08	1.12	0.11	0.42	0.31	1.75
RUNX2	Mean	1.60	0.97	1.44	1.41	1.34	1.16	1.45	1.04
	SD	0.21	0.20	0.07	0.28	0.20	0.22	0.26	0.31
OCN	Mean	-	2.95	-	3.84	-	3.22	-	3.95
	SD	-	2.03	-	0.73	-	1.54	-	2.32

At this stage, the effect of AGE-breakers on expression of alkaline phosphatase. osteocalcin, Runx2 and col1a1, and on mineralization is determined (Milestone 5).

Task 10. Data analysis, publications, reports. (Month 29-30.)

10a. Presentation/discussion at a CDMRP-required meeting or an orthopaedics-related conference.

A CDMRP-required meeting did not take place during the funding period. Although we did not have data in the form of a presentable abstract, we did discuss our methodologies and findings with other researchers at the Annual Meetings of the Orthopaedic Research Society (2013, 2014, 2015). As a result, we did modifications to our cell culture and analysis methods as explained above.

10b. Analysis of data

Based on the results presented in Task 2, we conclude that treatment of demineralized (Figures 2-4, 6-8) and undemineralized bone (Figures 10-11) with ALT-711 crosslink breaker causes chemical changes in the tissue.

Statistical Analysis of Mechanical Test Data (Aim 1)

Prior to the primary analyses, tests were performed to examine the effect of specimen geometry on the mechanical test variables and to verify that variations in geometry variables did not counfound the test groups.

Linear regression models and the untreated specimens were used to examine the effect of specimen thickness, notch asymmtery and notch eccentricity on the R-curve variables. The results suggested that K_{max} ($p<0.05$) increased with increased specimen thickness. No effect of specimen thickness was observed on K_0 ($p=0.2137$), Δa_{max} ($p=0.1772$), or R ($p=0.2626$). In addition, no effect of notch eccentricity or notch asymmetry was observed on any of the R-curve variables ($p<0.1767<0.9566$).

In order to examine if the treatment groups were different in terms of specimen geometry, repeated measures ANOVA was used, with Treatment as the repeated effect. The results indicated no difference in specimen thickness, notch eccentricity or notch asymmetry between treatment groups ($p>0.05$ for all). Due to the results of these preliminary examinations, the specimen geometry variables were not considred this point forward.

The main factors considered in the study were Treatment, Sex and Age, with the primary interest in Treatment. Therefore, for the primary analysis, mixed models were considered with one of R-curve variables (K_0, Δa_{max}, K_{max} or R) as the outcome and the following variables as effects:

Treatment:	Control, Glycated, ALT, Gly+ALT (Repeated)
Sex:	Male, Female (Fixed)
Age:	Young, Old (Fixed)
Donor:	Subject (Random)

All outcome variables, except K_0 were nonnormally distributed as tested by Shapiro Wilk W tests. Due to the nonnormality of the distributions, a Box-Cox transformation was applied to all variables prior to analysis [14]. The transformation was of the form $X^{(\lambda)}=(x^{\lambda}-1)/\lambda\gamma^{\lambda-1}$ ($\lambda\neq0$) or $X^{(\lambda)}=\gamma \ln(x)$ ($\lambda=0$), where γ is the geometric mean of the untransformed variable x. An optimal value of the transform parameter (λ) was determined for each variable so as to minimize sum of square of errors around the mean. All transformations are such that the transformed parameter increases with increasing untransformed parameter. All variables were normal after the transformation ($p>0.19$ to $p>0.99$).

Analysis started with examination of interactions. If significant interactions were found, separate models were run in subgroups. If interactions were not significant, the models were reduced to main effects and rerun. The procedure was iterated until all nonsignificant terms were removed and the final model results are reported. The level of statistical significance was set as $p<0.05$. The statistics package JMP (v10, SAS Institute, Cary, NC) was used for all analyses.

RESULTS: K_0, K_{max} and R were not significantly different between age, sex or treatment groups ($p>0.06$ for all) (Table 10). A marginal effect of age on K_0 ($p=0.078$) and treatment on K_{max} ($p=0.060$) could be observed (Figure 25). A significant three-way interaction of age, sex and treatment was found for Δa_{max} ($p<0.04$). When

the data were separated by groups, the effect of treatment was significant in old females ($p<0.04$), but not significant in old males ($p=0.072$), young males ($p>0.16$) or young females ($p>0.44$) (Figure 26). Post-hoc analysis revealed that ALT-treated group had a significantly greater Δa_{max} than the normal control group in old females.

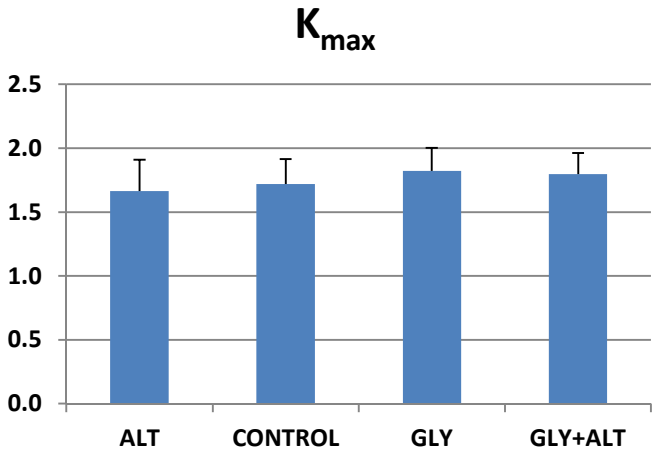

Figure 25: Maximum crack resistance among treatment groups. Differences were not significant ($p=0.060$). Note that the error bars represent within-subject standard deviations which take into account the repeated nature of the measurements (Cousineau, 2005).

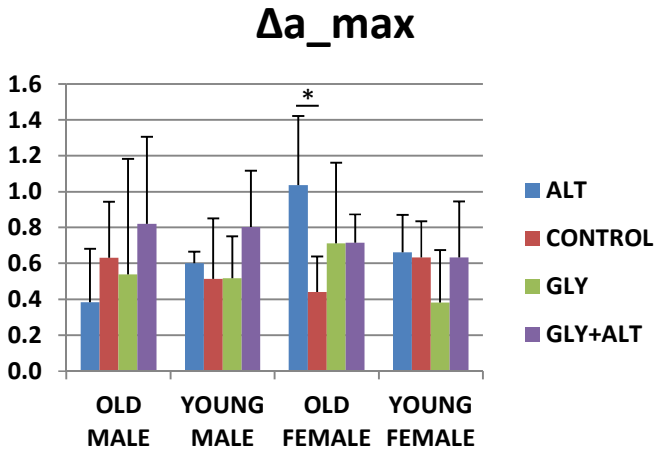

Figure 26: Crack extension when K_{max} is reached. ALT-treated group has a significantly greater Δa_{max} than the normal control group in old females (*). Note that the error bars represent within-subject standard deviations which take into account the repeated nature of the measurements (Cousineau, 2005).

Table 10. Summary of the statistical procedure and results for the mechanical test data. The entries (NS) show the sequence of elimination for the nonsignificant results. The numeric entries show p-values for the final model with the variable. Due to the significant 3-way interaction in $\Delta a_{max,}$ the data were split in age and sex groups and then analyzed separately. The last row summarizes the results of post-hoc analysis.

	K_0	Δa_{max}	K_{max}	R
Age	p=0.0783		NS5	NS5
Sex	NS6		NS6	NS6
Age * Sex	NS2		NS3	NS3
Treatment	NS5		p=0.0607	p=0.4079
Age * Treatment	NS4		NS2	NS4
Sex * Treatment	NS3		NS4	NS2
Age * Sex * Treatment	NS1	p=0.0335	NS1	NS1
Post-hoc Tukey		Old Female (p=0.0352) ALT > CNT		

Statistical Analysis of Cell Division, Apoptosis and Mineralization Data (Aim 2)
%Div, %Apop and %Min.Ar were nonnormal ($p<0.0001$ for all). Normal distributions could be obtained for %Div through a Box-Cox ($p=0.2267$) and for %Apop through a double inverse hyperbolic transformation ($p=0.5494$). Repeated measures ANOVA models followed by Tukey's post-hoc tests were used for the analysis of transformed %Div and %Apop variables. %Min.Ar was severely left skewed and could not be transformed to obtain a normal distribution. Friedman's nonparametric repeated measures ANOVA models were used followed by Steel-Dwass post-hoc tests for the analysis of %Min.Ar.

Treatment did not have a significant effect on %Div ($p=0.0911$) or % Apop ($p=0.1552$). Treatment effect was significant on %Min.Ar ($p<0.04$) with the ALT group being greater than the GLY+ALT group ($p<0.05$). Although not significantly different from others, the untreated and glycated groups were between the ALT and GLY+ALT groups (Figure 27).

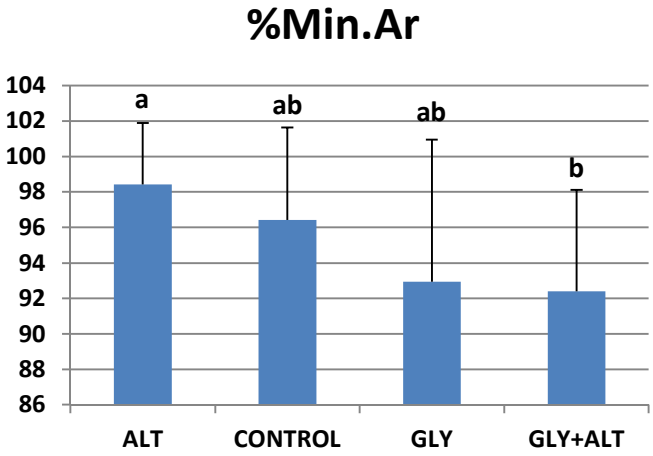

Figure 27: Mineralization differences among treatment groups. The data suggest that glycation and ALT have opposite effects on normal bone, reaching a significant level between ALT and GLY+ALT groups. Note that the error bars represent within-subject standard deviations which take into account the repeated nature of the measurements (Cousineau, 2005). These error bars would be different from those plotted in the descriptive graphs (Figure 24a). Bars not sharing a letter are significantly different.

When separated by sex, treatment effect was significant for %Div ($p<0.02$) in females but not in males ($p=0.7652$ and $p=0.3434$, respectively) (Figure 28). Cells on the glycation treated substrates (GLY and GLY+ALT) expressed a significantly less division than those on untreated control substrates.

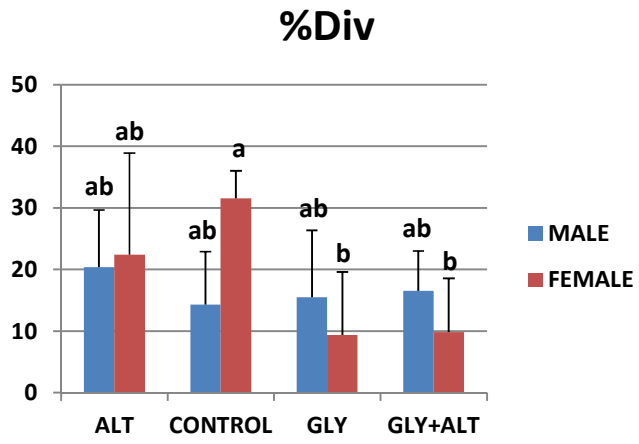

Figure 28: Differences in cell division. Cells on the glycation treated substrates (GLY and GLY+ALT) expressed a significantly less division than those on untreated control substrates in females only. Note that the error bars represent within-subject standard deviations which take into account the repeated nature of the measurements (Cousineau, 2005). These error bars would be different from those plotted in the descriptive graphs (Figure 21b). Bars not sharing a letter are significantly different.

When separated by age, treatment effect was significant for %Apop ($p<0.05$) in the young group but not in the old group ($p=0.9153$ and $p=0.6856$, respectively). Cells on the glycation treated substrates (GLY) expressed a significantly greater apoptosis than those on untreated control substrates (Figure 29). ALT treated groups (ALT and GLY+ALT) were between the untreated and GLY groups but were not statistically different.

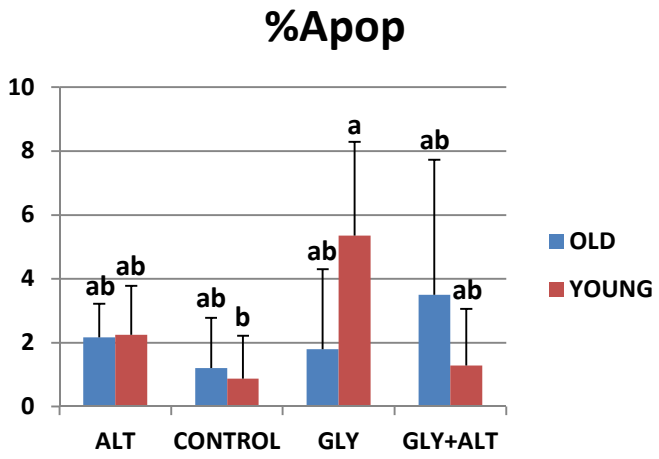

Figure 29: Percentage of apopotic cells is generally low. Nonetheless, cells were more apoptotic on glycated bone substrates than on untreated bone substrates from young donors only. Note that the error bars represent within-subject standard deviations which take into account the repeated nature of the measurements (Cousineau, 2005). These error bars would be different from those plotted in the descriptive graphs (Figure 22c). Bars not sharing a letter are significantly different.

When the data were further separated by both sex and age, RMANOVA tests were significant for %Div in old females ($p<0.05$); however, potentially due to loss of power, post-hoc tests revealed no significant difference between treatment groups.

Statistical Analysis of PCR Data (Aim 2)

The PCR variables were adjusted such that increasing values of the variable was associated with increasing levels of expression. Duplicate measurements from a sample were averaged and reduced to one data point. Two-way ANOVA was used for the analysis of ALPH, COL1A1 and RUNX2 with treatment as a four level nominal variable (ALT, GLY, ALT+GLY and PBS) and duration of cell culture as a two level ordinal variable (7 and 14 days). One-way ANOVA was used for OCN for which only one time point was measured. Post-hoc analyses were performed using Tukey's test (treatment) and t-test (culture duration). Fold increases were log transformed (base 2), essentially converting the data to $\Delta\Delta$CT for statistical analysis [15].

Both treatment and cell culture duration were significant in ΔCT ($p<0.0001$ for both), $\Delta\Delta$CT relative to PBS control ($p<0.0001$ and $p<0.0005$, respectively) and $\Delta\Delta$CT relative to no substrate ($p<0.0001$ for both) for ALPH, but the treatment effect did not depend on duration ($p>0.12$) (Figure 30). Post-hoc tests indicated that glycation treated groups (GLY and GLY+ALT) were greater than non-glycation treated groups (ALT and control). All variables were greater at day 14 than day 7.

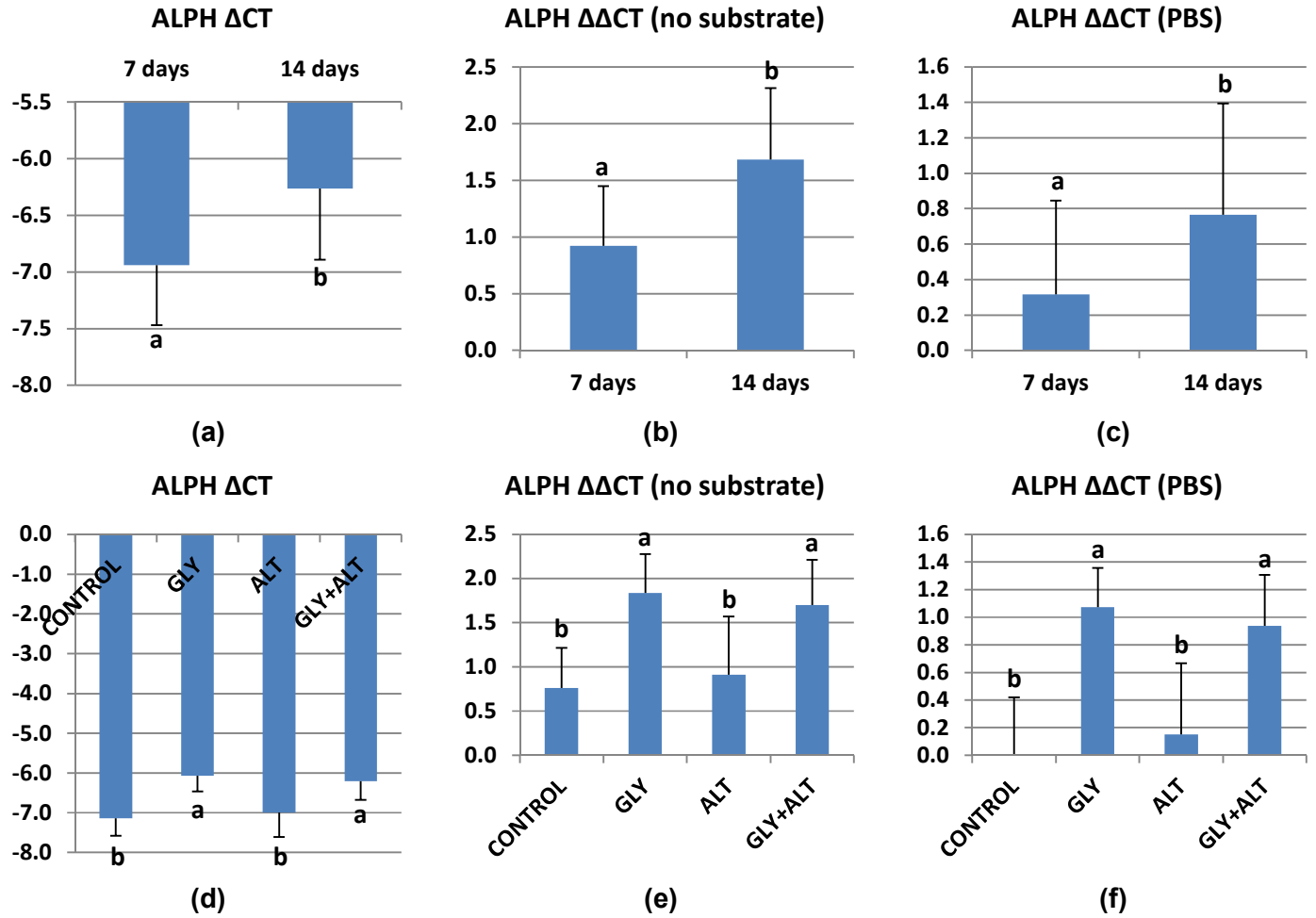

Figure 30: Expression of alkaline phosphatase by culture duration (a-c) and treatment (d-f) as calculated relative to an internal control (a, d), relative to nonbone substrate (b, e) and relative to untreated bone substrate (c, f). Bars not sharing a letter are significantly different.

Treatment was significant in ΔCT, ΔΔCT relative to PBS control and ΔΔCT relative to no substrate ($p<0.002$ for all) for COL1A1 (Figure 30). Cell culture duration was significant for ΔΔCT relative to no substrate ($p<0.0001$), with the values being greater at day 14 than day 7, but was not significant for ΔCT ($p>0.16$) or ΔΔCT relative to PBS control ($p>0.11$). ALT treated specimens had significantly greater values than GLY and GLY+ALT groups. Although not significantly different, the control group was between the ALT and GLY/GLY+ALT groups.

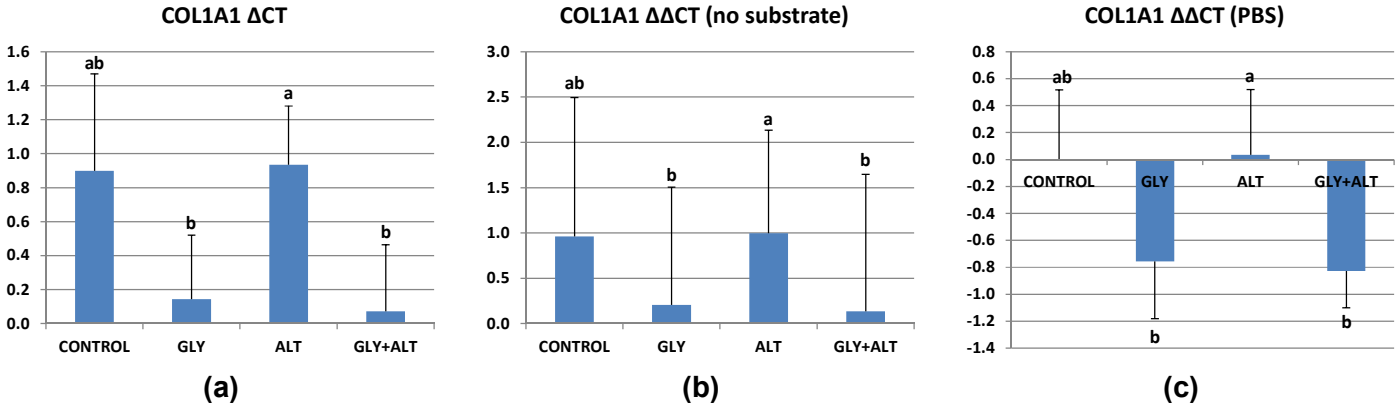

Figure 31: Expression of COL1A1 by treatment as calculated relative to an internal control (a), relative to nonbone substrate (b) and relative to untreated substrate (c). Bars not sharing a letter are significantly different.

Duration of cell culture was significant in ΔCT ($p<0.0001$) and ΔΔCT relative to no substrate ($p<0.0008$) but not in ΔΔCT relative to PBS control ($p>0.15$) for RUNX2. The values for ΔCT were greater at day 14 than at day 7 while the trend was reversed for ΔΔCT relative to no substrate (Figure 32). Treatment was not significant in any variable for RUNX2 ($p>0.66$).

No significant treatment effect was found for OCN ($p>0.61$).

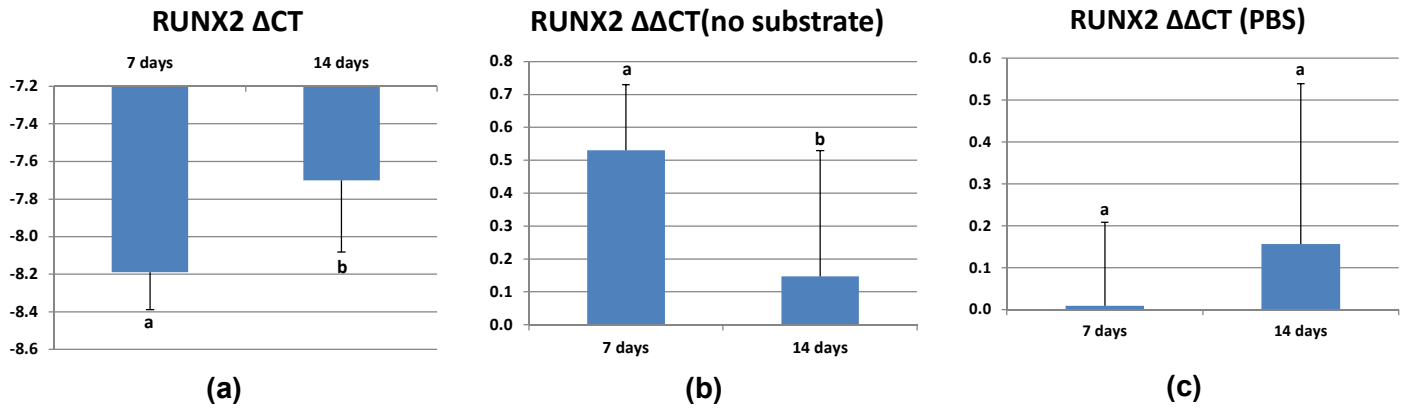

Figure 32: Expression of RUNX2 by treatment as calculated relative to an internal control (a), relative to nonbone substrate (b) and relative to untreated substrate (c). Bars not sharing a letter are significantly different.

DISCUSSION

Although not statistically significant, there was a trend for glycation to increase crack propagation toughness (K_{max}) and for ALT to reduce this in untreated control and glycated bone. It may be possible to demonstrate these effects with an increased sample size and establish that ALT has an effect opposite to that of glycation. However, it must be noted that the observed trends are counterintuitive given the literature data suggesting that glycation decreases crack propagation toughness [16, 17]. However, this assertion has not been directly tested in previous studies using an R-curve approach. Several other studies failed to find an appreciable effect of nonenzymatic crosslinks on bone's mechanical properties [18, 19]. The current results suggest, if anything, glycation induced crosslinks, just like enzymatic crosslinks [20, 21], may be mechanically beneficial. A previous study examining a crosslink breaker (PTB) similar to ALT711 found that PTB reverted the effects of glycation on postyield strain of cancellous bone using a small sample of male subjects only [22]. We found that the effect of the ALT crosslink breaker is complexed with donor sex and age in cortical bone. Specifically, we found that critical crack length increases in ALT treated normal bone for old females. This indicates an ability for old female bone to tolerate longer cracks before they become catastrophic. Without an accompanying increase in crack resistance, the direct mechanical significance of this behavior is unclear. On the other hand, the crack length tolerated in the tissue may have important effects on bone remodeling driven by microdamage, thereby having an indirect effect on bone mechanics. The ability of ALT to affect untreated bone but not glycated bone suggests that the AGE products introduced into the bone matrix through artificial glycation in ribose are different from those accumulate naturally. The finding that critical crack length is affected by a crosslink breaker in old females only further suggests a fundamental difference in the organization of the extracellular matrix between old women and others. However, the nature of these differences are currently unknown.

Cell differentiation and maturity were achieved on all substrates as the substrates were eventually almost fully mineralized. Percentage of the mineralized area tended to be higher in ALT treated normal bone than untreated bone while percent mineralization tended to be lower in glycated bone samples than in untreated samples, resulting in a significant difference between ALT treated normal bone and ALT treated glycated bone. It seems that the AGE products introduced by artificial glycation can reduce the mineralization but this effect is not reversed by ALT. Rather, ALT tends to increase mineralization in normal bone. These results, once again, suggest an important difference between AGE products that accumulate naturally and those that are introduced artificially. The reduced cell division and increased apoptosis in glycated samples are consistent with a negative effect of AGEs on bone formation. That these effects depend on age and sex supports the suggestion that a fundamental difference in the age-dependent changes in the organization of the extracellular matrix between

men and women.

The temporal relationships for ALPH, COL1A1 and RUNX2 expression, provided by the ΔCT variable were more consistent with the literature [23-25] than those provided by the ΔΔCT variables. As expected, ALPH and RUNX2 increased from 7 to 14 days as measured by ΔCT. COLA1 is expected to increase and then decrease within this period and therefore a nonsignificant difference from 7 to 14 days is not surprising. We measured osteocalcin at day 14 only because osteocalcin is considered a product of mature osteoblastic cells. The levels of OCN expression were low at this time point as would be expected prior to full maturation of the cell. Although ALT's effect on RNA expression does not appear to be universal across all markers and GLY treatments, the COL1A1 results suggest that ALT has an effect opposite to that of glycation on normal bone. The ALPH results suggest increased osteogenic activity when artificially glycated bone is used as substrate. This is in contrast to expectations from cell culture experiments that did not use bone substrates. This set of results again suggest that the type of AGE occurring in naturally aged bone and that in artificially aged tissue is different. Nonetheless, the histology and PCR results collectively suggest that glycation increases osteogenic activity at earlier stages of cell differentiation but this effect is not carried forward to affect bone mineralization.

The spectrophotometry and fluorescence microscopy results indicate that the ALT crosslink breaker does affect the composition of extracellular bone matrix. Artificial glycation, as expected, increased the AGE content of the bone and ALT partially reversed this effect. However, the current results do not support a direct involvement of AGEs in the reduction of bone's crack resistance as the trends appeared to be favoring glycation. In terms of mechanical performance and cell behavior, the action of artificial aging and reversal by ALT appeared to be dependent on the nature of the AGEs present in the tissue. The results further suggest that artificial glycation in ribose may not accurately represent the naturally occurring AGEs in bone tissue. As such there is not a uniform effect of cross-link breaker on all tissue types, which would prohibit its use as an enhancement method for all allografts.

10c. Preparation and submission of manuscripts to peer-reviewed journals.
10d. Writing of grant proposals to pursue the hypotheses developed by the current project.

The current report will serve as the first draft of a manuscript to report the findings. The current findings require modification of our original hypothesis that ALT-711 enhances both mechanical and osteogenic properties of all allograft cortical bone. Due to the somewhat different scope of the future direction and the need for development of additional research tools and new preliminary data to address the new questions, a grant application has not been completed during the funding period. ***(Milestone 6.)***

10e. Writing of final reports.
Annual reports have been submitted and approved. Submission of the current report completes this task. ***(Milestone 7.)***

PROBLEMS ENCOUNTERED

The acquisition of cadaveric human tissues took considerably longer time than anticipated. This was despite initiating protocols with three tissue donation agencies. The original time estimate was based on previous experiences with the tissue banks; however due to a number of factors tissue acquisition has become more challenging in recent years. We have been able to acquire the approved amount of tissues and prepared them for the final tests before the end of the funding period. However, towards the end of the original funding period (2/19/2014), we were notified by the Headquarters, US Army Medical Research and Materiel Command (HQ USAMRMC) Office of Research Protections (ORP) that the Biological Resource Center (BRC) is under investigation by the Arizona Attorney General (AAG) and the FBI. We were instructed to halt research involving specimens from this cadaveric specimen supplier and quarantine the tissues until a decision was made.

Tissues acquired through one of the agencies (Platinum) turned out to be sourced through BRC and accounted for about 40% of our total cadaver material in this project. We requested a no-cost extension in order to finish the work with the non-BRC specimens while providing additional time to work with the BRC specimens in case that a decision to proceed with them was made. We received approval from the ORP for continuing to use the BRC material on 6/12/2014 after which the research proceeded.

4. KEY RESEARCH ACCOMPLISHMENTS

We developed experimental protocols for treatment of demineralized and undemineralized bone samples and accompanying quantification methods using both spectroscopy and/or epi-fluorescence microscopy.

We found evidence that ALT-711 can reduce levels of AGEs induced by ribose.

We found that glycation affects osteogenic properties of bone using human bone tissue, rather than model tissues, as substrates.

We found evidence that ALT affects the mechanical and osteogenic properties of bone.

We also found that the effect of ALT is selective between young vs old donor age, male vs female source and naturally vs. artificially induced AGEs. These complex interactions make the use of ALT for the originally proposed purpose (enhancement of allograft bone) difficult. However, they offer a new research avenue for understanding the disparate increase of bone fragility with age in women compared to men.

5. CONCLUSION

Currently allograft is the only practical source of bone grafts but it carries a plethora of issues such as nonunion due to poor bone quality as they are often sourced from old donors. One of the main contributing factors for poor bone quality is thought to be a natural accumulation of AGEs (advanced glycation endproducts) which forms non-enzymatic crosslinks that results in brittle and biologically poor bones. It was proposed that once the crosslinks can be broken artificially by ALT-711, this will improve mechanical properties and create favorable bone matrix for the stem cells that will eventually result in a better integration of bone in patients.

In the supported period, we established evidence that the crosslink breaker ALT-711 can modify bone matrix, affect the mechanical behavior of bone during fracture and affect the behavior of stem cells during osteoblastic differentiation. However, the mechanical performance of the treated bones and the osteogenic activity of stem cells on treated substrates were not uniform enough that the proposed crosslink breaking method can be translated into a protocol for enhancement of allograft performance. In order to achieve this goal, a better understanding of the different types of naturally occurring AGEs and how they affect bone biology and mechanics is needed. Our data suggest that AGEs formed by incubation with ribose differ substantially in their effect on the mechanical performance of bone and their effect on the ability of bone substrates to support osteogenic differentiation of stem cells than naturally occurring AGEs. It is also possible that more effective crosslink breakers are needed to selectively remove the relevant AGEs from the tissue.

While not a direct objective of the research carried out, we acquired valuable information challenging the current understanding of glycation effects on bone mechanics and biology. The intriguing finding that age related accumulation of AGEs and their manifestation on bone's crack resistance and remodeling vary between sex groups may be key to understanding age related bone fragility and the disparity in fracture risk.

6. PUBLICATIONS, ABSTRACTS, AND PRESENTATIONS

a. No reportable outcome in terms of manuscripts, conference presentations or funding applied based on the work supported by this award is available at this time.

b. Presentations
"Glycation End Products and Fracture Mechanics of Femoral Bone: What can a Crosslink Breaker Do?"
Bone and Joint Center Seminar Series, Henry Ford Hospital, Detroit, Michigan, May 30, 2014.

7. INVENTIONS, PATENTS AND LICENSES

Nothing to report.

8. REPORTABLE OUTCOMES

Nothing to report.

9. OTHER ACHIEVEMENTS

Employment or research opportunities applied for and/or received based on experience/training supported by this award

This project provided training opportunities for the following individuals whether or not they were compensated by the project funds:

1. Woong Kim, PhD: University of Auckland, New Zealand, Post-doc fellow, 2012 – 2014.
   RT-PCR analysis, sample procurement and preparation, fluorescence microscopy and fluorescence quantification, glycation+ALT-711 treatment, fracture toughness analysis.

2. Richard Banglmaier, PhD: Wayne State University, Senior Research Engineer, 2012-2013.
   Fluorescence quantification using spectrophotometry

3. Daniel Oravec, MSc: Tampere University of Technology, Finland, Senior Research Engineer, 2012 – present
   Specimen procurement, accounting, machining, mechanical test system, microscopy image analysis.

LIST OF PERSONNEL RECEIVING PAY FROM THE RESEARCH EFFORT

Yener N. Yeni
Gary Gibson
Daniel Oravec
Liang Zhang

10. REFERENCES

1. Wu, Z., A.J. Laneve, and G.L. Niebur, *In vivo microdamage is an indicator of susceptibility to initiation and propagation of microdamage in human femoral trabecular bone.* Bone, 2013. **55**(1): p. 208-15.

2. Willett, T.L., et al., *In vitro non-enzymatic ribation reduces post-yield strain accommodation in cortical bone.* Bone, 2013. **52**(2): p. 611-22.

3. Karim, L., et al., *Differences in non-enzymatic glycation and collagen cross-links between human cortical and cancellous bone.* Osteoporos Int, 2013. **24**(9): p. 2441-7.

4. Gustafson, M.B., et al., *Calcium buffering is required to maintain bone stiffness in saline solution.* J Biomech, 1996. **29**(9): p. 1191-4.

5. Brown, C.U., Y.N. Yeni, and T.L. Norman, *Fracture toughness is dependent on bone location--a study of the femoral neck, femoral shaft, and the tibial shaft.* J Biomed Mater Res, 2000. **49**(3): p. 380-9.

6. Yeni, Y.N., et al., *The influence of bone morphology on fracture toughness of the human femur and tibia.* Bone, 1997. **21**(5): p. 453-9.

7. Saxena, A. and S.J. Hudak, *Review and extension of compliance information for common crack growth specimens.* International Journal of Fracture, 1978. **14**: p. 453–68.

8. Nalla, R.K., J.J. Kruzic, and R.O. Ritchie, *On the origin of the toughness of mineralized tissue: microcracking or crack bridging?* Bone, 2004. **34**(5): p. 790-8.

9. Malik, C.L., et al., *Equine cortical bone exhibits rising R-curve fracture mechanics.* J Biomech, 2003. **36**(2): p. 191-8.

10. Grasl-Kraupp, B., et al., *In situ detection of fragmented DNA (TUNEL assay) fails to discriminate among apoptosis, necrosis, and autolytic cell death: a cautionary note.* Hepatology, 1995. **21**(5): p. 1465-8.

11. Labat-Moleur, F., et al., *TUNEL apoptotic cell detection in tissue sections: critical evaluation and improvement.* J Histochem Cytochem, 1998. **46**(3): p. 327-34.

12. Atale, N., et al., *Cell-death assessment by fluorescent and nonfluorescent cytosolic and nuclear staining techniques.* J Microsc, 2014. **255**(1): p. 7-19.

13. Rasband, W.S. *ImageJ, U. S. National Institutes of Health, Bethesda, Maryland, USA, http://rsb.info.nih.gov/ij/, 1997-2014.* 1997.

14. Box, G.E.P. and D.R. Cox, *An Analysis of Transformations.* JRSS, 1964. **B26**: p. 211-43.

15. Livak, K.J. and T.D. Schmittgen, *Analysis of relative gene expression data using real-time quantitative PCR and the 2(-Delta Delta C(T)) Method.* Methods, 2001. **25**(4): p. 402-8.

16. Nyman, J.S., et al., *Age-related factors affecting the postyield energy dissipation of human cortical bone.* J Orthop Res, 2007. **25**(5): p. 646-55.

17. Nalla, R.K., et al., *Effect of aging on the toughness of human cortical bone: evaluation by R-curves.* Bone, 2004. **35**(6): p. 1240-6.

18. Reddy, G.K., *Glucose-mediated in vitro glycation modulates biomechanical integrity of the soft tissues but not hard tissues.* J Orthop Res, 2003. **21**(4): p. 738-43.

19. Willems, N.M., et al., *Higher number of pentosidine cross-links induced by ribose does not alter tissue stiffness of cancellous bone.* Mater Sci Eng C Mater Biol Appl, 2014. **42**: p. 15-21.

20. Oxlund, H., Barckman, M., Ortoft, G., and Andreassen, T. T., *Reduced concentrations of collagen cross-links are associated with reduced strength of bone.* Bone, 1995. **17**(4 Suppl): p. 365S-371S.

21. Banse, X., T.J. Sims, and A.J. Bailey, *Mechanical properties of adult vertebral cancellous bone: correlation with collagen intermolecular cross-links.* J Bone Miner Res, 2002. **17**(9): p. 1621-8.

22. Bradke, B.S. and D. Vashishth, *N-phenacylthiazolium bromide reduces bone fragility induced by nonenzymatic glycation.* PLoS One, 2014. **9**(7): p. e103199.

23. Safadi, F.F., et al., *Bone Structure, Development and Bone Biology*, in *Bone Pathology*, J.S. Khurana, Editor 2009, Humana Press: New York. p. 1-50.

24. Lian, J.B. and G.S. Stein, *Development of the osteoblast phenotype: molecular mechanisms mediating osteoblast growth and differentiation.* Iowa Orthop J, 1995. **15**: p. 118-40.

25. Lian, J.B., et al., *Regulatory controls for osteoblast growth and differentiation: role of Runx/Cbfa/AML factors.* Crit Rev Eukaryot Gene Expr, 2004. **14**(1-2): p. 1-41.

11. APPENDICES

No appendix material is included.